8-9-2014

PLANT-BIOMIMETIC HYDROGEL ACTUATORS: CREATING MOVEMENT IN HYDROGELS THROUGH THE STUDY OF PLANTS

Christen Rhodes
University of South Carolina - Columbia

PLANT-BIOMIMETIC HYDROGEL ACTUATORS: CREATING MOVEMENT IN HYDROGELS THROUGH THE STUDY OF PLANTS

by

Christen Rhodes

Bachelor of Science
James Madison University, 2012

Submitted in Partial Fulfillment of the Requirements

For the Degree of Master of Science in

Mechanical Engineering

College of Engineering and Computing

University of South Carolina

2014

Accepted by:

Wally Peters, Director of Thesis

Tarek Shazly, Reader

Lacy Ford, Vice Provost and Dean of Graduate Studies

DEDICATION

Thanks to my wonderful family and fiancé for all your love and support. It's been a roller coaster ride!

ACKNOWLEDGEMENTS

Special thanks to Dr. Tarek Shazly and his students, Dr. Jahid Ferdous and Boran Zhou, for sharing their lab space, equipment, and knowledge with us and to Katy Rutledge and Dr. Greg Harris of the Jabbarzadeh Research Lab for advice and equipment.

ABSTRACT

Plants are sessile organisms that have developed methods of movement to respond to environmental stimuli. Some of the approaches feature the unequal expansion of cells and controlling deformation direction through fibers under swelling and drying. Hydrogels are three dimensional polymer networks that have the capacity for large volume changes due their affinity for water and can be tough and/or stimuli-responsive. In this paper, three preliminary plant-biomimetic hydrogel actuator designs are discussed and tested from wet to dry. The first actuator design, termed a 1%-0.1% bilayer, features two layers of different swelling and drying rates due to differences in cross-linking density. When the 1%-0.1% bilayer actuator dries, it bends towards the 0.1% layer. The 1%-0.1% bilayer is designed to mimic the plant bending movement derived from the unequal expansion of cells. The second actuator design, called a random fiber bilayer, features one layer with short randomly oriented fibers in it and a second fiber-less layer. The random fiber layer restricts the amount of shrinking/swelling that can occur and results in bending around the fiber-less layer as drying occurs. The idea for this actuator is inspired by fiber orientation and movement in the wheat awn. The third actuator design, known as a perpendicular fiber bilayer, is designed to mimic fiber actuation principles derived from pine cone scales. Long fibers are aligned on one layer to be perpendicular to long fibers in the other layer. The fibers constrain deformation to perpendicular directions only; this results in bending along two axes due to the fiber

orientation in the two layers. All three of the designs testing from wet to dry is generally successful and these proof-of-concepts for translating plant movement principles to hydrogel actuators could be used to build more complex hydrogel actuators in the future.

TABLE OF CONTENTS

LIST OF FIGURES

LIST OF SYMBOLS

Wp	Peak Wattage of a Solar Cell
δ	The angle between the sun's rays and the equator.
ω	The angle parallel to the equator that measures between the sun rays and the location on Earth relative to the equator.

LIST OF ABBREVIATIONS

AIRS .....High-Aspect-Ratio Rigid Structure

BC .....Bacterial Cellulose

CPT .....Cloud Point Temperature

BZ Reaction .....Belouzov-Zhabotinsky Reaction

DGI .....Dodecylglyceryl Itaconate monomer

DIW.....Direct Ink Writing

DLP technology .....Digital Light Projection technology

DN hydrogel.....Double Network hydrogel

HAIRS..... Hydrogel High-Aspect-Ratio Rigid Structure

HAIRS-1 .....Hydrogel High-Aspect-Ratio Rigid Structure with nanocolumns detached

HAIRS-2 .....Hydrogel High-Aspect-Ratio Rigid Structure with nanocolumns attached

IPN hydrogel.....Interpenetrating Network hydrogel

LCE.....Liquid Crystal Elastomer

LCST hydrogel.....Lower Critical Solution Temperature hydrogel

LDM.....Low-temperature Deposition Modeling

MDM.....Multi-Nozzle Deposition Modeling

MFA.....Microfibril Angle

M-LDM.....Multi-Nozzle Low Temperature Deposition Modeling

MW ..... Molecular Weight

NC hydrogel.....Nanocomposite hydrogel

Pa..... Pascal

PAAm hydrogel ..... Polyacrylic Acid hydrogel

PAM.....Pressure Assisted Microsyringe

PAMPS hydrogel .....Poly(2-acrylamido-2-methylpropane sulfonic acid) hydrogel

PEG hydrogel.....Polyethylene Glycol hydrogel

PEG-DA hydrogel.....Polyethylene glycol diacrylate hydrogel

PGMA hydrogel.....Polyglycidyl Methacrylate hydrogel

pHEMA Hydogel..... Poly(hydroxyethyl methacrylate) hydrogel

PTFE .....Polytetrafluoroethylene

RPBOD System .....Rapid Prototyping Robotic Dispensing System

SGC.....Solid Ground Curing

SLA.....Stereolithography

SMART.....Self-Regulated Mechanochemical Adaptively Reconfigurable Tunable

SWCN..... Single-Wall Carbon Nanotubes

TFSC..... Thin Film Solar Cell

UCST hydrogel..... Upper Critical Solution Temperature hydrogel

UV light .....Ultraviolet Light

v/v .....Volume Percent Concentration

μ-SLA .....micro-stereolithography

2D.....Two Dimensional

2PP .....Two Photon-Polymerization

3D.....Three Dimensional

3DP^{TM} Technology .....3D Printing Technology

Chapter 1 - INTRODUCTION

The inspiration for this research came from observing plants and how they track the sun throughout the day to increase their solar efficiency. The idea of building a solar cell that mimicked a plant's solar collection methods jumpstarted an exploration of research that started with how plants move and ended with hydrogel actuators. It was a truly fascinating journey.

The literature survey started first by examining the reasons why tracking the sun with solar cells might be important. Next, the current methods of passively tracking the sun using traditional photovoltaic cells were examined to see if someone had already created a biomimetic passively tracking photovoltaic cell. Research revealed there were no effective, smart designs, so subsequently the focus shifted to current solar technology. Thin film solar cells (TFSCs) were examined due to their flexibility and thin profile which is similar to a leaf, the "solar cell" of a plant. TFSCs that were flexible and could be applied to any substrate without a significant decrease in efficiency were discovered in the literature [1].

Research next shifted to determining exactly how sessile (stationary) plants achieve movement. Many methods were found from research articles; methods using unequal expansion of cells, changes in turgor pressure, cohesion forces, and soft swell-able matrices embedded with fibers [2]. The last method became the focus of research; the effect of embedding stiff fibers in a material that has high swelling and shrinking rates can be seen in many parts of plants, such as pine cone scales, wheat awns, and trees

[2, 3, 4, 5]. Research continued into current bio-inspired passive tracking solar panels that already existed in the literature and a thin film solar cell that tracked the sun using photo-thermomechanical liquid-crystal elastomer nanocomposite was found [6].

After investigating how plants move and the current bio-inspired passively tracking solar cells, the research moved onto find a suitable material. The material needed to swell and shrink a large amount and have the ability to have fibers embedded within it. Hydrogels were quickly discovered as a promising material. A thorough examination of research was conducted to determine exactly what they were as well as their synthesis, classification, and mechanical properties. An exciting survey of literature revealed various types of tough and stimuli-responsive hydrogels, fibers and bilayers hydrogels, hydrogel actuators, rapid-prototyped hydrogels, and hydrogels with the ability to perform transpiration.

Once a survey of literature was completed, the next step was to choose a hydrogel with which to create the actuators. A polyethylene glycol diacrylate (PEG-DA) hydrogel with photoinitiator 2-hydroxy-2-methylpropiophenone that started cross-linking under ultraviolet (UV) radiation was chosen due to its relatively simple formula and quick synthesis. Three actuator models based on plant principles were designed so that they had the ability to translate to a variety of hydrogels, which might be tough or stimuli-responsive. The goal was to make hydrogel actuator models that could be applied to any hydrogel and prove plant-based movement concepts that could be used in the future to create more complex actuators. The purpose of this research was not to make a hydrogel actuator that only worked with the specific PEG-DA hydrogel. All hydrogel specimens were made in molds that yielded a rectangular specimen of 25 x 13 x 2.4mm. The first

model, called a 1%-0.1% bilayer, was based on bending driven by different shrinking rates across two layers, similar to a bimetallic; this was very similar to plant movement driven by unequal expansion of cells. The different shrinking rates in the bilayer were caused by variations in cross-linking densities resulting from changes in photoinitiator concentrations. The second model, commonly termed random fiber bilayer in this paper, introduced another bilayer model with one layer of randomly oriented short fibers and another layer without fibers. This model was inspired by the wheat awn and its layer of randomly oriented fibers along its appendages. The randomly oriented fibers caused the fiber layer to shrink less than the fiber-less layer, resulting in bending towards the fiber-less layer. The third model, called a perpendicular fiber bilayer, had long fibers that spanned the whole length of the hydrogel. This model idea was directly derived from plant movements in a pine cone scale. The fibers ran parallel to the 13mm edge in one layer and parallel to the 25mm edge in the other layer. This constrained the hydrogel to move only in the direction perpendicular to the fibers, resulting in overall bending along both the short 13mm axis and the long 25mm axis. All models displayed the predicted behavior when allowed to go from a wet to dry state. Some cracking and splitting did occur, sometime correlating with no bending, especially in the 1%-0.1% bilayer case.

Many great opportunities for further research in the area of plant-biomimetic hydrogel actuators still exist. The hydrogel actuators need to be studied further to find out the precise mechanics of what is going on, especially at the interface between layers. The retention of shape as the hydrogel goes from dry to wet needs to be examined as well as any cyclic fatigue that might occur as the specimens are loaded and unloaded. Also, hydrogels actuators could be made with fibers and rapid prototyping into complex

shapes. The hydrogel used for these actuators is not limited to PEG-DA; hydrogels that are tough or stimuli-responsive could be used. Stimuli-responsive biomimetic hydrogel actuators would be especially interesting as they would not rely on the amount of water in the environment for their volume change. Finally, future research could examine the fibers and their stiffness, surface roughness, quantity, distribution and orientation, and the effect of chemically binding fibers to the hydrogel.

Chapter 2 – A LITERATURE REVIEW

2.1 SOLAR CELLS AND TRACKING

2.1.1 Increasing Energy Efficiency through Solar Tracking

Photovoltaic solar cell produce on a yearly average about only 20% of their peak wattage (abbreviated W_p) found in laboratory controlled conditions (the conditions are an intensity of 1000 W/m^2, temperature of 25°C, and the source of the light is at 42° relevant to the horizon). Major sources of this inefficiency are variations in incident solar radiation due to time of day/night and cloud cover. The Earth orbits around the sun in an ellipse and rotates at a tilt, which means that angle of the sun's rays always changes with time. The angle between the sun's rays and the equator is called δ and can be seen in Figure 2.1 below.

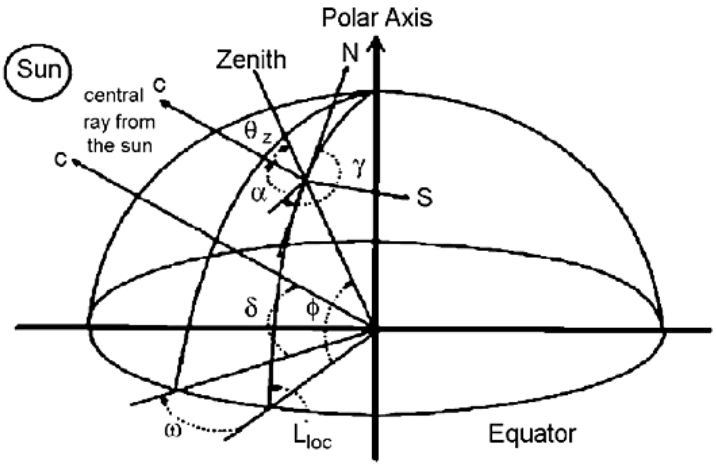

Figure 2.1 Diagram of Solar Angles based on the Equator and Sun [7]

The angle δ will be zero at the autumn and spring equinoxes. The angle that measures along the equator the distance between the sun rays and the location on Earth is termed ω and can also be seen in the Figure 2.1 below. This angle will be zero at noon [7].

The optimal angle for the sun's rays to hit a solar panel is 90°. However, since most photovoltaic panels are fixed in place, this means that a lot of energy is lost due to the inability to track the sun. Mousazadeh et al. state that the amount of energy gained when tracking systems are used may be as high as 57% based on simple calculations [7]. When designing a solar tracking system, there are two options. One option is to design it to track on one axis; these designs may track in the equatorial (focusing on angle ω) direction or azimuth/elevation tracking (focusing on angle δ). The two axis tracking system uses both equatorial and azimuth/elevation tracking methods. It is not necessary for the tracking angle of a solar panel to be highly accurate; even panels that were off by 10° were still able to collect 98.5% of the extra energy gathered from tracking. There are two types of solar tracking methods; passive and active. Active tracking methods use some of the energy collected by the solar panel to track the sun. Passive tracking methods do not and are traditionally based on shape memory alloys or thermal expansion of matter. Currently, there are many more active than passive tracking systems. Mousazadeh et al. has a great review of current passive and active solar tracking technologies [7].

2.1.2 Thin Film Solar Cells

Traditional photovoltaic cells have been largely limited over the years by their bulkiness and rigidity. Recent research into thin film solar cells (abbreviated TFSCs), however, is promising, especially with the new developments by Lee et al. concerning a

TFSC that can be applied to any substrate without loss of 7.5% efficiency [1]. The efficiency is also unaffected by flexure as well. The TFSC was fabricated on a Si/SiO_2 wafer that had been thinly coated with nickel, seen in Figure 2.2 (a) below.

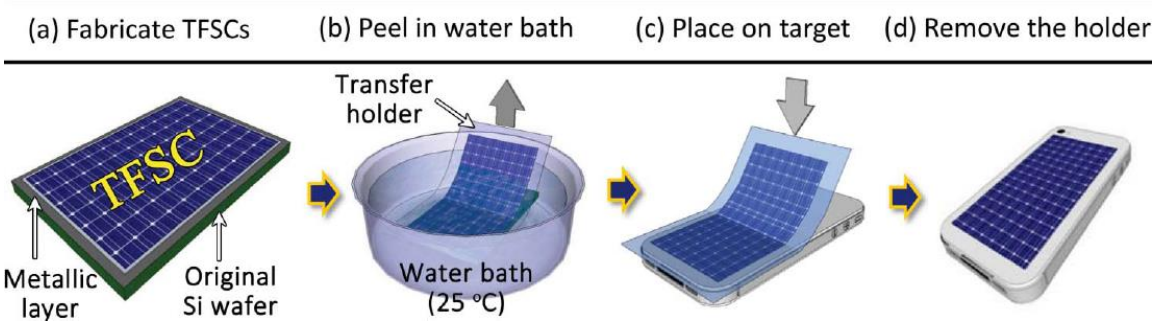

Figure 2.2 Peel and Stick TFSC Manufacturing Process (a) TFSC fabricated on the silicon wafer over thin nickel layer (b) TSFC placed in water bath and peeled from the silicon as a result of water-assisted subcritical debonding of the Nickel SiO_2 interface (c) Application of the heated TFSC to the substrate using a common adhesive (d) Removal of the thermal release tape on top of the TFSC [1]

A transparent thin layer of ProTek® was then laid on top of the TSFC to protect it from the thermal release tape that was applied on top of that. The TFSC was then placed in a water bath at 25°C and an edge of the thermal release tape was peeled up to allow water to penetrate the assembly and react with the thin nickel layer and SiO_2, which resulting in subcritical debonding, allowing the TFSC to separate from its silicon wafer. This can be seen in Figure 2.2 (b). The TFSC was then heated to 90°C to allow the thermal release tape to be loosened and applied to the desired surface with a common adhesive, seen in Figure 2.2 (c). The loosened thermal release tape was then removed, seen in Figure 2.2 (d). Lee et al. state that the TFSC can be attached to any substrate regardless of its material properties, rigidity, and flatness [1].

2.2 INSPIRATION FROM THE PLANT WORLD

2.2.1 What is Biomimetics and Biomimicry?

Biomimetics, also known as biomimicry, occurs when humans use nature's solution to a similar problem as a baseline or inspiration for a solution to their own problems [8, 9]. Examples where scientists and engineers examined the natural world for inspiration are becoming more and more common as information becomes more available across disciplines. Engineers and designers may seek to mimic how nature has designed specific materials, the mechanics or dynamics of a certain process or movement, the structure of certain aspects of an organism, and even form and shape to deliberately evoke a connection to nature or a specific reaction [8]. An example of an application of biomimicry would be the adhesive developed by Geim et al. which mimicked how a gecko's feet adhered to a surface through micrometer hairs and van der Waals forces [10]. So when trying to build a passive tracking solar cell, it becomes a natural progression to look for inspiration from nature. The immediate solution is to look at plants; after all, plants essentially have small solar cells built into their leaves.

2.2.2 Movement in Sessile Organisms

Plants track stimuli and respond with movement all the time, whether the directional stimulus (or vector) is gravity, water, mechanical, or the sun. A tropism is the growth response of a plant to a directional stimulus and its intensity, which could also be termed a stimulus vector in some cases [11]. Thigmotropism is the response of the plant to a mechanical stimulus vector, gravitropism is the response to the gravity stimulus vector, hydrotropism is the response to water or the water potential, and phototropism is

the response to the light stimulus vector. Most of these occur over days or even months, such as phototropism. Some plants, however, track and respond to light daily. If the flower tracks and follows the sun it is called floral heliotropism, which can be seen in the snow buttercup *Ranunculus adoneus*. The cells on the shaded side of the flower stem, known as the peduncle, experienced greater rates of elongation than those on the sunny side of the plant, resulting in a bending towards the sun [12]. If the daily tracking of the sun occurs in the movement of the leaves, it is called paraheliotropism if the plant bends its leaves parallel to the sun vector and diaheliotropism if the leaves move so that they are perpendicular to the light vector. The mechanism of the movement for these leaves is the pulvinus located at the base of the petiole, or leaf, and it essentially acts like a hinge as turgor pressure changes [13]. It has also been shown that the concentration of certain solutes in the transpiration stream can greatly affect the turgor pressure changes in the pulvinus and subsequently the leaf movement [14, 15].

Plants are often seen as static, or sessile, organisms; in contrast to animals, they cannot move away from changing conditions or threats because they have no muscles. In spite of this, or perhaps because of it, plants have developed a number of mechanisms to allow them to move in relatively short amounts of time. Burgert et al. cites four different mechanism of movement for plants [2]. Most movements are often combinations of these different mechanisms. The first of these mechanisms is unequal cell expansion which results in a bending movement. The second mechanism is a turgor pressure change in motor cells that actuates a movement. An example of this might be the guard cells found around the stomata that control the gas exchange within the leaf. The pulvinus is another example of a motor cell for the movement of leaves in paraheliotropism and

diaheliotropism, as discussed earlier. The Venus fly trap is also theorized to operate on this principle as is the reaction to touch (mechanical stimulation) by leaves of *Mimosa pudica*. The third mechanism relies on the cohesion force that can be found in water and essentially uses a slingshot mechanism by forcing bending through cohesion. Water is removed from a series of linked cells until the force of cohesion is overcome and the cell shoot back into their original shape. This mechanism is often used to disperse spores and the spores are flung out of the plant when the cells shoot back into their original shape. The last mechanism is cell wall swelling or shrinking [2]. The walls are embedded with single crystal 2.5nm cellulose fibers that are coated by a thin layer of hemicellulose [2, 3, 5]. The hemicellulose allows for a good connection between the fibers and the highly swellable matrix which they are embedded in. This matrix is called lignin [3]. The angle of the fibers relative to the cell axis is call the microfibril angle (abbreviated MFA) and this is the most important part in determining what direction the cell will swell in as a result of an increase in humidity or exposure to water [2]. The cell will swell in an anisotropic manner; swelling, or deformation, will be allowed in the direction perpendicular to the fibers but not parallel to them due to the fact that the fibers will not deform. This results in an anisotropic deformation. Figure 2.3 on the next page demonstrates this by showing how fiber direction can dictate how the cell will respond to an outside force. The fibers are shown as grey and the soft matrix as white. In part A), we see no significant deformation occurring in response to an outside force where as in part B) we see the deformation of the soft matrix as the fibers offer little reinforcement relative to the direction of the applied stress. Part C) demonstrates what might happen

should the force occur in a direction that is neither perpendicular or parallel to the fibers and the shearing that may occur between the fibers and matrix as a result.

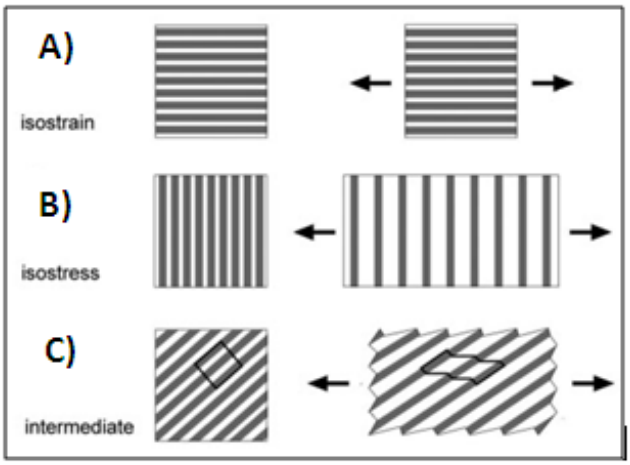

Figure 2.3 Fibers(shown as grey lines) embedded in a malleable matrix (shown as white) and the fiber angle influence on cell response to an outside force or stimulus: (A) The cell experiences isostrain and negligible deformation due to rigid fibers running parallel to outside force (B) Isostress is experienced by the cell as the soft matrix deforms since the fibers offer no support due to the fact that they are perpendicular to the external force (C) A combination of isostrain and stress is experienced as the cell deforms due to the fact that the fibers are neither parallel nor perpendicular to the external force [4].

The cell wall swelling or shrinking is considers to be a passive actuation mechanism by the authors Burgert at al.; in other words, whether or not the cell is alive, this mechanism will continue to function when exposed to different level of humidity [2]. Cell wall layers and sections can account for various plant movements and functions.

In trees, the secondary cell walls may have up to four layers that have varying MFAs. Figure 2.4 on the next page demonstrates the typical wall layers found in a tree cell.

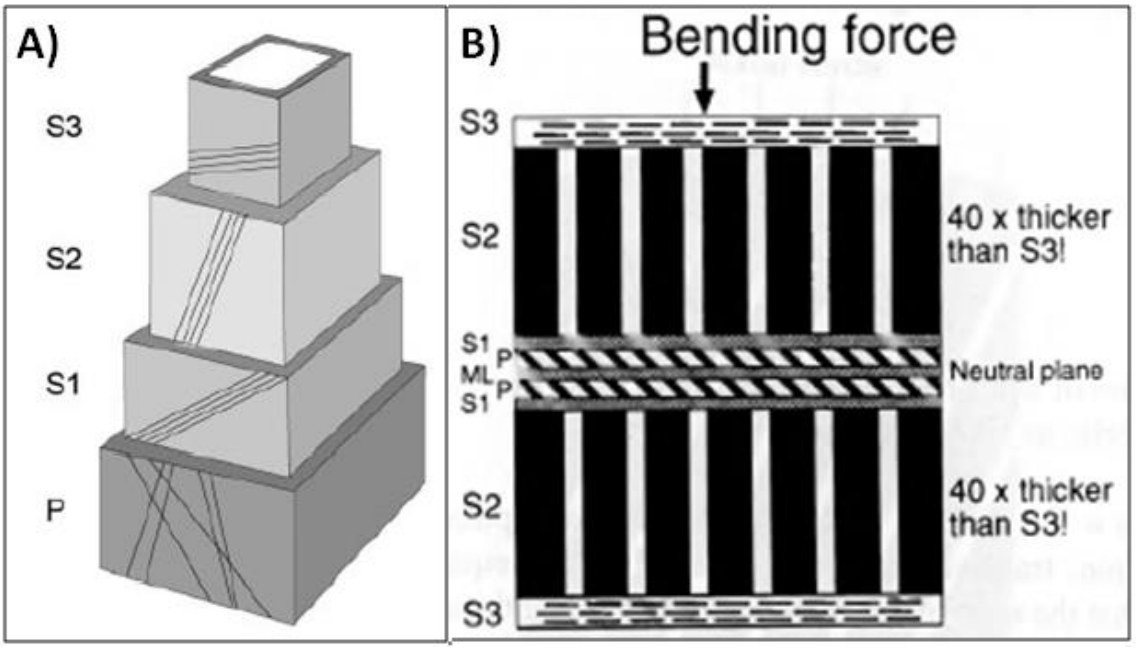

Figure 2.4 Cell Wall Layers and Typical Direction of Fibers for Trees: (A) 3D Model of the cell wall of a tree and its layers [11] (B) Top down view of the layers of a cell wall and the direction of the fibers [3]

The layer furthest in on the interior of the cell is termed the S3 layer. The function of this layer is to resist collapse caused by the transpiration forces that occur within the cell [3]. As such, the MFA in this layer is very large and almost perpendicular to the cell axis. The next layer is termed the S2 layer and its function is to support the tree. It is forty times thicker than the S3 layer and the MFA may change 0° to 60° depending on where the cell is located in the tree and where the tree is in its lifecycle [3, 4]. This layer is always roughly perpendicular to the S3 layer. A smaller MFA will mean a higher modulus of elasticity; this is commonly seen in mature trees that are stiffer or in cells that are experiencing compressive forces, such as the bottom of a branch. These cells will fail comparatively faster once yielded. A higher MFA will mean more flexibility and a large plastic deformation after yielding; this can be seen in younger trees or in cells

experiencing tension forces, such as the top of a branch. The final layer is the S1 layer. The function of the S1 layer is to prevent radial expansion that might occur under compression and as such it has microfibrils that are approximately parallel the S3 Layer and are perpendicular to the S2 layer. The primary cell wall (labeled P in the diagrams) surrounds the secondary wall and has fiber oriented randomly throughout; this means that it will swell in an isotropic manner when exposed to water. The principles of the S2 layer show that a cell, if torsion is assumed negligible and the volume is constant, will experience a negative strain, or shortening, along the cell axis direction when exposed to water if the MFA is <45° and a positive strain, or lengthening, along the cell axis direction if the MFA is >45°. In other words, cells made for compression will actually lengthen when exposed to water and cells made for tension will actually axially contract when exposed to water [3, 4]. This can be seen in Figure 2.5 below.

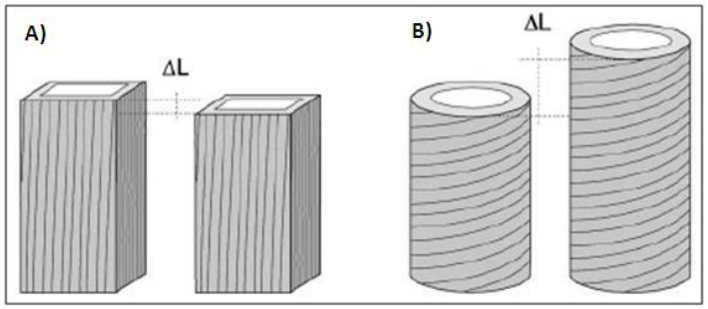

Figure 2.5 Effect of MFA in the S2 layer on the cell's response to water: (A) Cell where the S2 layer contains fibers at a MFA <45° experience a negative ΔL or shortening (B) Cell where the S2 layer contains fibers at a MFA >45° experience a positive ΔL or lengthening [4]

The concept of orienting fibers differently in different parts of the plant to actuate various movements is also seen in wild wheat awns. Wheat awns are essentially a seed

with two appendages, or awns, extending out from the seed to form a v-shape, seen below in Figure 2.6.

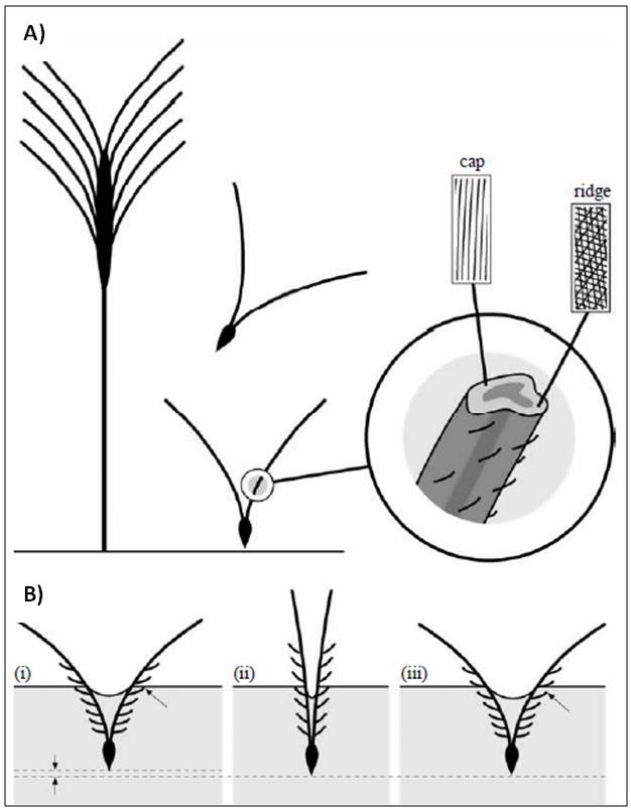

Figure 2.6 Diagram of a Wheat Awn and how it moves using fibers and humidity change: (A) Wheat awn with V shaped appendages and the round T with fibers being distributed randomly in the ridge and parallel relative to the overall length of the appendage in the cap (B) Demonstration of how the wheat awn digs itself into the soil using the daily humidity changes (i) Day (ii) Night (iii) Day [4]

The appendages are in the shape of a rounded T, with the top part of the T being labeled the cap and the bottom part of the T being labeled the ridge. The cap faces inwards towards the other appendage and the ridge faces outwards. The ridge also has small hairs

attached to it that point up and away from the seed. The cap has fibers running parallel to the longitudinal appendage axis and the ridge has layer of fibers that alternate at angles approximately perpendicular to each other. Consequently, an anisotropic swelling in the direction perpendicular to the appendage longitudinal axis is seen in the cap when night falls and humidity increases and a isotropic swelling perpendicular to the fibers is seen in the ridge. This, combined with bending that occurs from the moisture change from night to day results in a swimming motion. The bending results from the two different orientations of fibers in the appendages. The swimming motion, termed hygroscopic motion, causes the wheat awn seed to dig deeper and deeper into the soil as the V formed by the appendages continually contracts and expands due to the unequal swelling in the cap and ridge of the awns. The hairs on the ridge keep the wheat awn from rising up towards the soil's surface [4, 16].

Pine cones are another example where the deliberate orientation of fibers in different parts of the plant realizes actuation. In conifer cones, the goal is to have pine cone scales open as they dry out, releasing seeds. The scales consist of essentially two layers, seen in Figure 2.7 on the next page. The inner layer of the scale contains fibers that are oriented parallel to the longitudinal scale axis and the other layer contains fibers oriented perpendicular to the scale axis. The first layer limits expansion in the longitudinal scale direction and the second layer allows it; the result of this is a bending when the pine cone is wet as the fibers cause the layers to deform at different rates and in different directions. The layer on the bottom shrinks more than the top layer along the longitudinal scale axis, which results in the pine cone opening; this can be seen on the right side of Figure 2.7 C) and D). When the pine cone is wet, both layers swell but the bottom layer swells more

than the top layer along the longitudinal scale axis due to the direction of its fibers and thus the pine cone scale bends towards its top layer and closes; this can be seen on the left side of Figure 2.7 A) and B) [2, 5]. This mechanism of actuation is analogous to that of a bimetallic material [5].

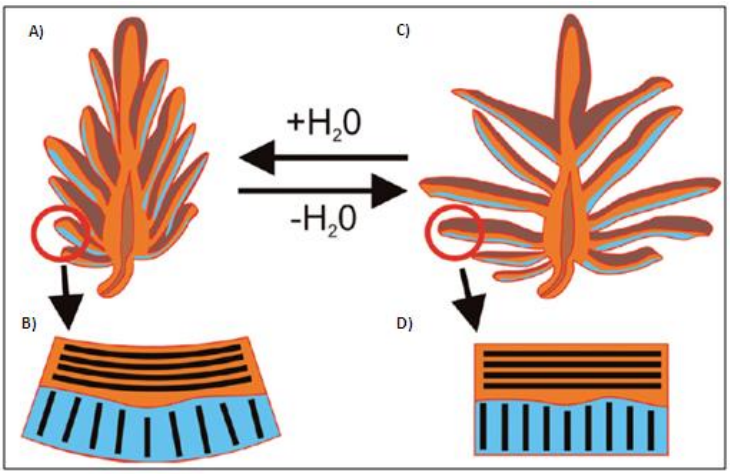

Figure 2.7 Response of pine cone scale to moisture [5]

2.2.3 Current Bio-inspired Solar Panels

Currently, there is only one prototype of a passive bio-inspired solar tracking panel. This panel was developed by Li et al. and uses a photo-thermomechanical liquid-crystal elastomer nanocomposite [6]. The solar cell is set up on a horizontal platform that is supported by three to four pillars. Each of these pillars contained an actuator, a reflective polymer film concave mirror to concentrate heat and light, and a PTFE elastic support. The actuator sits right at the focal point of the polymer mirror and is made of liquid crystal elastomer (abbreviated LCE) embedded with single-wall carbon nanotubes (abbreviated SWCN) to enable good conversion of photon energy into thermal energy and enhanced conduction through the LCE. The LCE nanocomposite also contains a

network of polyurethane fibers as well to strengthen the material. If the temperature is above the nematic-isotropic transition temperature for the LCE, then the actuator will contract. This means that the actuators in the pillars facing the sun's rays will contract and the pillars on the other side of the platform will not; resulting in a tilting of the platform and solar panel towards the direction of the sun. This actuation mechanism is inspired by the heliotropism principle of the snow buttercup *Ranunculus adoneus*. This plant, as mentioned earlier, practices floral heliotropism through unequal cell elongation which results in bending. The researchers were able to achieve a steady state position with the prototype around 110 seconds after exposure to outside light. The angle ranges that were achieved ranged up to a 60° altitude angle and 180° azimuth angle. In some cases, the photocurrent was increased by more than a 100% [6].

2.3 FIBER EMBEDDED HYDROGELS AS BIOMIMETIC ACTUATORS

2.3.1 What are hydrogels?

Hydrogels consist of synthetic or natural polymer three dimensional networks that are cross-linked and may swell by absorbing remarkable amounts of water (when compared to their dry weight) due to certain environmental stimuli. The three dimensional structure of the hydrogel in its swollen state is due to the hydrophilic groups in the polymeric network [17, 18]. The original environmental stimuli for hydrogels to swell was the presence of water but researchers have now been able to make them respond to changes in pH, temperature, ionic strength, electric fields, presence of enzymes and so on [17]. A hydrogel can be characterized as chemical, physical or a combination of both physical and chemical; a physical hydrogel, also known as a reversible hydrogel, occurs when the network is held together by molecular forces, ionic

bonding, hydrogen bonding, hydrophobic interactions, or some combination of the previous options. These processes may be reversible. A chemical hydrogel, also known as a permanent hydrogel, occurs when covalent bonds hold the cross-linking of the network together; these bonds are irreversible and thus the network is irreversible. This means the degree of swelling for chemical hydrogels is controlled by the hydrophilic polymers in the network and their interactions with the water as well as the amount of cross-linking that has occurred [18, 19]. Both chemical and physical hydrogels have issues with homogeneity, especially around the edges of the hydrogel or molecule because of free chains that have not bonded [20].

2.3.2 Types of Hydrogel Synthesis

There are many methods of preparation for hydrogels. It is important to remember that once the hydrogel is formed from its components, it is one molecule [17]. The change from separate components into one molecule is called the sol-gel transition or gelation [18]. Physically cross-linked hydrogels may be formed through heating and cooling, ionic interactions, complex coacervation, H-bonding (hydrogen bonding), maturation, and freeze-thawing. Examples of hydrogels formed from heating and cooling are gelatin (typically derived from collagen in many animal byproducts) and carrageenan (extracted from red seaweeds) solutions. The hot solution results in random coil configurations of the polymers when above the transition temperature and forms a gel as the liquid is cooled due the formation of helices from the random coil configuration as well as other junction zones that may form and aggregate with other helices [18]. The process of physical hydrogel formation is diagramed in Figure 2.8 on the next page.

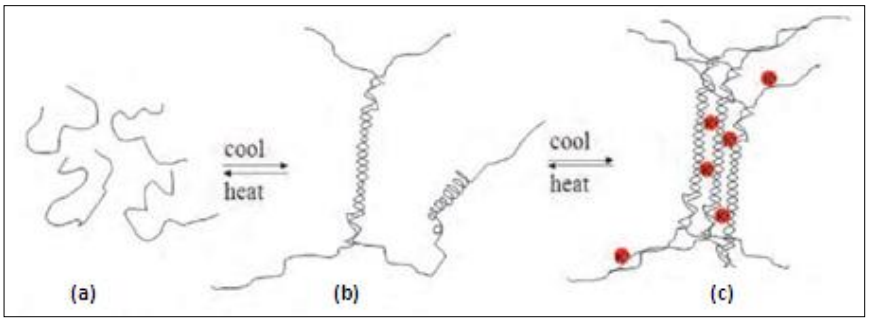

Figure 2.8 Physical Hydrogels formed through heating and cooling: (a) Polymer chains upon heating (b) Polymer helices interlocking with each other (c) Further bonds or forces that may develop in the presence of certain molecules like ions, shown as red circle [18]

Hydrogels formed from ionic interaction occur when counterions (ions that will maintain electric neutrality of molecules) are added to ionic polymers and effectively aggregate the polymer chains together through crosslinking. This is the top hydrogel formed in Figure 2.9 below, which is termed an "Ionotropic" hydrogel [20].

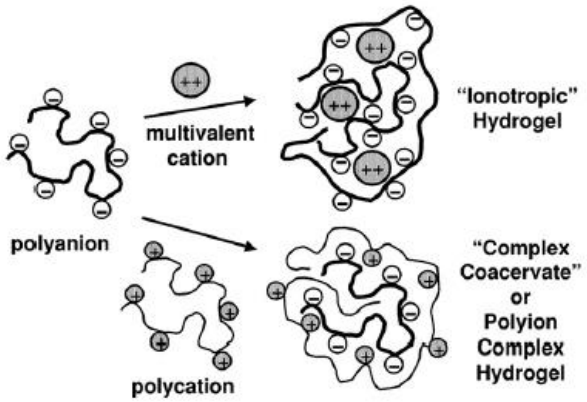

Figure 2.9 Difference between hydrogels formed from counterions (top) and coacervate hydrogels (bottom) [20]

The counterions may have a valence of two or three. Complex coacervation occurs when polymers have a negative charge (termed polyanion) are combined with positively charged polymers (termed polycation) to form a gel. This is the bottom hydrogel in Figure 2.9 on the previous page.

H-bonding usually occurs when the pH of the solution is modified to encourage bonding with functional groups on the polymer, which are typically carboxyl groups. The maturation process is diagrammed below in Figure 2.10.

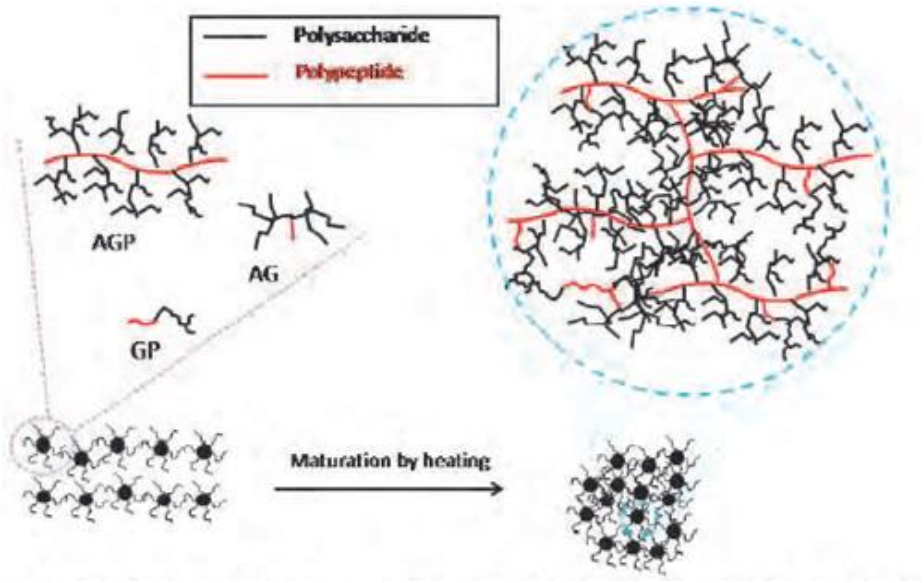

Figure 2.10 Maturation: Items to the left of the arrow are the constituents of the hydrogel with different molecular weights and protein amounts which form the molecule or hydrogel on the right side of the arrow due to the addition of heat [18]

Maturation, sometimes termed heat induced aggregation, is usually used for gum based hydrogels (such as those made from gum arabic, gum ghatti, and Acacia kerensis), which contain multiple constituents of different molecular weights and protein content that

eventually aggregate together to form a hydrogel when exposed to heat. In this diagram, the constituents of different weight and protein eventually aggregate into one single molecule (the hydrogel) as a result of the addition of heat.

Hydrogels formed by freeze-thawing are repeatedly frozen and thawed, allowing for crystal formation in the solution. Eventually these crystals form the gel. A crosslinking agent may not be needed for some of these gels, allowing for greater biocompatibility in medical applications [18, 21].

Chemically cross-linked hydrogels are formed either through chemical cross-linking or through grafting. When hydrogels are chemically cross-linked, the polymer chains are linked through the addition of a cross-linking agent that covalently bonds with the polymer chains. When hydrogels are grafted, an existing polymer is treated to form active surfaces that can then be cross-linked with monomers. Figure 2.11 below shows the basic grafting process.

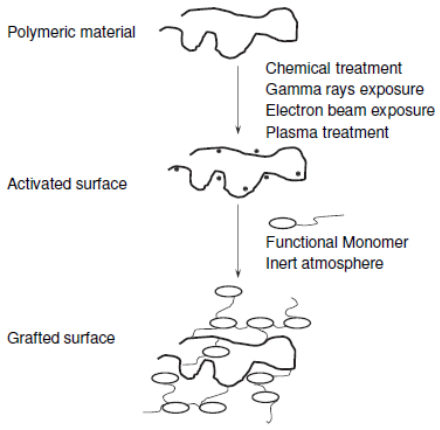

Figure 2.11 Grafting Process [18]

The active surfaces on the polymer may be formed through chemical methods, which means a chemical reagent is added to allow the crosslinking, or through radiation methods. Radiation grafting involves high energy radiation that leads to free radicals (which are molecules, ions, or atoms with an open electron shell) that then lead to polymerization [18].

Radiation cross-linked hydrogels are made through aqueous state, paste, and solid state radiation. Aqueous state radiation occurs when polymers in a diluted solution are irradiated and the radiation is mainly absorbed by water, resulting in free radicals, and a hydrogel is formed. Radiation in paste occurs when the number of polymers in solution is relatively high and thus the radiation produces free radicals from both the solution and the polymer and a hydrogel is formed. Solid state radiation occurs when a hydrogel forms from the generation of free radicals and macroradicals from the moisture and the macromolecules respectively [18].

2.3.3 Hydrogels Classification by Precursor Components

Hydrogels may also be classified based on the components from which they are synthesized. There are three main types of this classification; synthesis from monomers, prepolymers, and polymers, seen in Figure 2.12 on the next page.

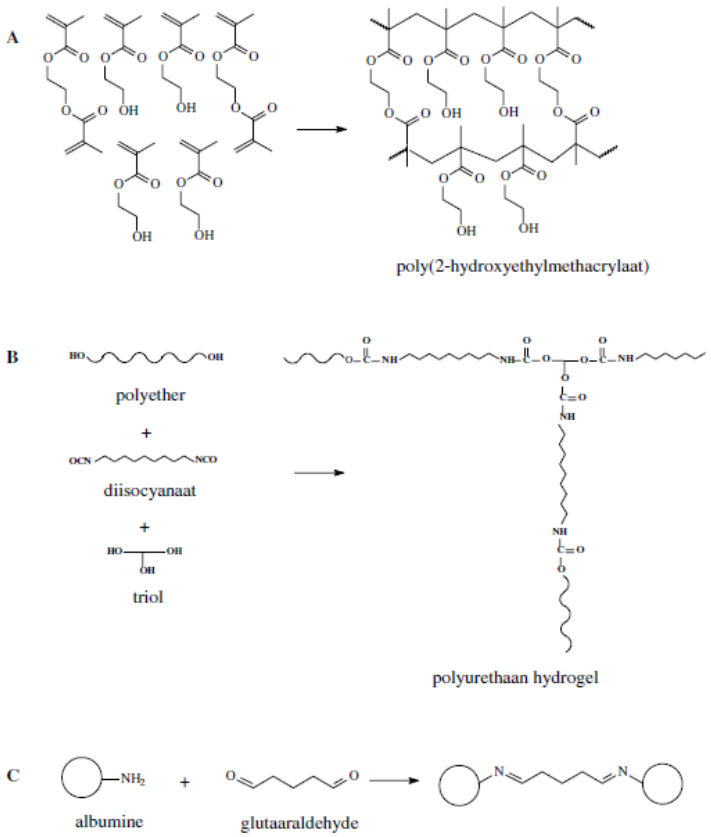

Figure 2.12 Different components from which hydrogels may be synthesized: A) Monomers B) Prepolymers C) Polymers. [22]

Monomers are molecules of low molecular weight that may be combined with other molecules of low molecular weight to form a polymer. Synthesis from monomers occurs when hydrophilic monomers are copolymerized with polyfunctional (one or more functional group) monomers acting as cross-linkers. Hydrogels synthesized from this technique have been used as contact lenses as well as electrophoresis gels [22].

Prepolymers are monomers, or systems of monomers (sometimes called oligomers), that have been modified to have an intermediate molecular weight.

Prepolymers, also known as polymer precursors, can form polymers. Synthesis from prepolymers occurs when the prepolymers are cross-linked together [22].

Synthesis of hydrogels from polymers occurs when the polymers are cross-linked. The crosslinking may be chemical or physical. Gels that are physically cross-linked can later be modified to be chemically cross-linked. An example of a polymer synthesized hydrogel would be gelatin and agarose (usually derived from seaweed) cross-linked together [22].

2.3.4 Mechanical Properties of Hydrogels

Hydrogel research has predominantly focused on the food industry and biomedical engineering applications, such as for tissue repair and regeneration [19]. This is primarily due to the characteristics of some hydrogels such as a high water absorption capacity, biodegradability, water permeability, and biocompatibility [17, 18]. Hydrogels are often compared to a less dense rubber [23, 24].

A hydrogel's mechanical properties may be determined from tensile testing. The hydrogels are usually cut in their swollen shape into dumb-bell shapes and then may or may not be immersed in a solution kept at a specified temperature as they are stretched [23]. It is important to note that hydrogels may take up water or exude it when subjected to tension or compression. As hydrogels swell, their mechanical properties, such as modulus, strength, and extension, typically decrease. Hydrogels are most commonly tested in compression tests as rectangular or cylindrical specimens; however, researchers must be very careful with these tests because of the possibility of inducing hydrostatic compression from the shearing forces that may occur at the platelet-hydrogel interface. It

is important to pay attention to whether the literature reports compressive or tensile strengths [23, 24].

Mechanical properties of hydrogels may be manipulated a number of ways but the three most common methods are through altering the composition, cross-linking density, and the synthesis conditions. The precursor components of a hydrogel may lend their mechanical properties to the final hydrogel. If a stronger hydrogel is needed, increasing the amount of a strong precursor component would most likely increase the strength [23].

The cross-linking density also affects the mechanical properties of a hydrogel; typically the most significant effects occur in the strength and swelling ability. The easiest way to change the cross-linking density is through the amount of cross-linking agent (if a cross-linking agent is used). A more densely cross-linked hydrogel will have higher strength but it will swell less and therefore have lower diffusivity rates [23].

The conditions under which the hydrogel is synthesized may also greatly affect the mechanical properties. Temperature and reaction time may affect the cross-linking that occurs. Also, the solvent in which the precursors components are immersed can greatly impact the final hydrogel as well by affecting the shape of the precursors [23].

2.3.5 Tough Hydrogels

In the past, application of hydrogels has largely been limited by the low strength of the material. However, recent efforts have brought about a new type of hydrogel, termed "tough hydrogel." There are six major types of tough hydrogels: interpenetrating network (often termed IPN), double network (abbreviated DN), ionically-crosslinked networks, nanocomposite (abbreviated NC), slide ring or "slip-link," topological, and microsphere, or microcomposite, hydrogels [25]. Some hydrogels may combine a number

of these methods together. IPNs are a broad term and typically define any hydrogel that is made of two or more cross-linked networks that intertwine with each other, seen in Figure 2.13 a) below.

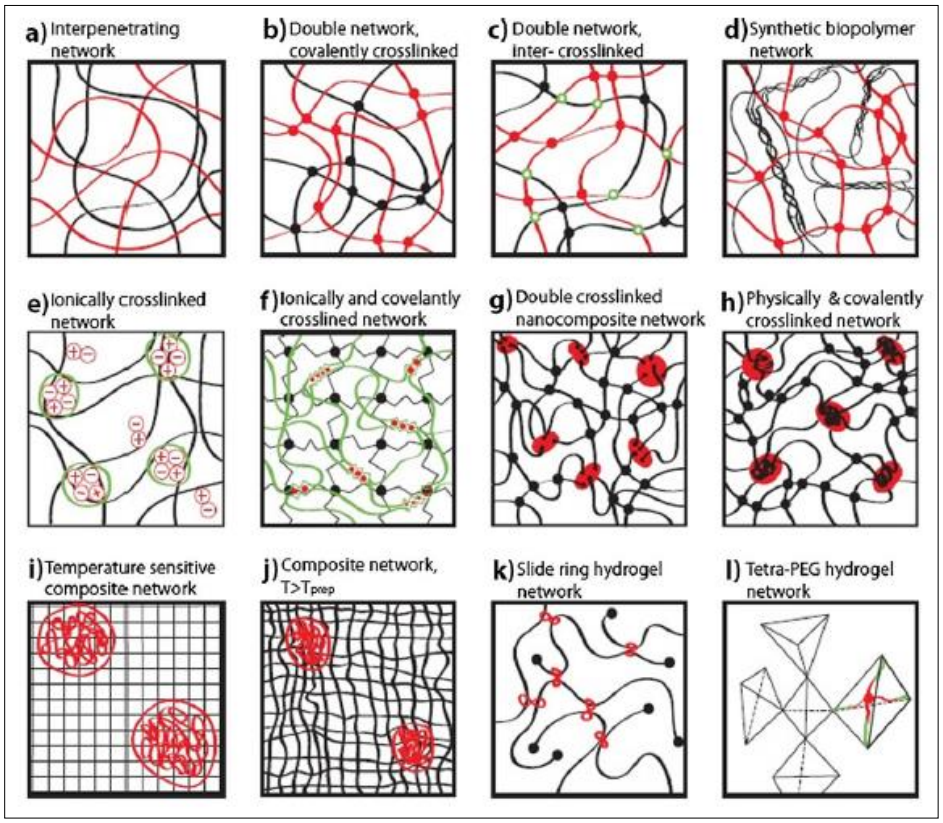

Figure 2.13 Common types of tough hydrogels [25]

DNs can be considered to be a specific type of IPN; in the 2013 review on tough hydrogels by Peak et al., the authors state that a DN hydrogel consists of two IPN hydrogels that are *covalently* cross-linked. These hydrogels are usually synthesized by making the first hydrogel and then soaking it in a solution of the second before crosslinking again, seen in Figure 2.13 b) above. It is possible for crosslinks to develop between the first and second network as well, which would be termed an inter-crosslinked DN and can be seen Figure 2.13 c). The first network in a DN will have a

tighter cross-linked structure than the second and may act as sacrificial bonds to be broken for the dissipation of energy in the event of force application. Once broken, these bonds may not be re-formed. DN tough hydrogels of poly(2-acrylamido-2-methylpropane sulfonic acid) (PAMPS) and polyacrylic acid (PAAm) have been known to have 17 MPa engineering compressive strength[25, 26]. DN hydrogel have sometimes demonstrated strain hardening from interactions between the networks, such as hydrogen bonding. IPNs may also contain natural polymers, such as collagen, in an effort to enhance biocompatibility and/or biodegradability for biomedical applications, seen in Figure 2.13 d). One of the most interesting hydrogels synthesized recently using a natural polymer was a DN hydrogel with jellyfish gel and PAAm, capable of tensile stresses of up to 40 MPa [25, 27].

Another type of tough hydrogel is an ionically cross-linked hydrogel which mimics the structure of an IPN hydrogel and can be seen in Figure 2.13 e). A single polymer network is ionically cross-linked twice. Hydrogels of this type have been shown to have engineering compressive fracture stresses of around 1 MPa. A common variation of this method is to make a hydrogel that features a combination of covalent and ionic crosslinking networks, seen in Figure 2.13 f). A great application of this method is a tightly ionically cross-linked first network intertwined with a looser covalently cross-linked second network; this allows for an energy dissipation mechanism with the first network when an external force is applied that isn't quite strong enough to break the covalent bonds in the second network. Self-healing occurs when the hydrogel is unloaded as the ionic bonds re-form. A PAAm and alginate-Ca^{2+} gel featuring this method was

stretched to over 20 times its original length, fractured at 156 kPa, and was said to be "notch-insensitive" [25, 28].

NC gels feature nano-sized platelets, molecules, or materials to which multiple polymer chains often attach either through covalent or physical crosslinking, seen in Figure 2.13 g) and h); exfoliated silicate nanoplatelets (otherwise known as clay) is most commonly used [29, 25]. NC hydrogels of materials other than silica that have acted as multifunctional crosslinkers include graphene nanosheets, and hydroxyapatite nanoparticles [25, 30]. A DN NC gel of PAMP, PAAm, and silica nanoparticles was able to resist fracture up to 73 MPa [25, 31].

Hydrogels may also be microcomposites, with either microgels or microspheres, seen in Figure 2.13 i) and j). Microspheres are micro- or nano- scaled spheres of stimuli responsive microgels, which can be made from hydrogels or porous polymers. These spheres, like the nanoparticles in NC gels, can be multifunctional. Microcomposite DN gels of poly(N-isopropylacrylamide) and poly(vinyl amine) have been found to have engineering compressive stresses of up to 30 MPa [25, 32].

Slide ring hydrogels, seen in Figure 2.13 k), may be known as "slip-link" or "pulley-chain" or topological hydrogels. The defining aspect of these hydrogels is that the cross-links, which are in the shape of figure eights, may move, or slip, along linear polymer molecules and are kept from slipping off the linear molecule by bulky end molecules [29, 33, 25, 34]. This effect allows for viscoelastic behavior as well as increased toughness, stretching, and swelling [29, 33]. As the hydrogel is stretched, the crosslinks slide, allowing for more stretching and uniform distribution. These hydrogels have been stretch to 1,000% original length before fracture [33, 25, 34].

The last common type of tough hydrogel is a Tetra-Polyethylene Glycol (abbreviated as PEG) hydrogel, which feature few network defects and entanglements seen with more linear polymer network hydrogels due to their comparatively more homogenous gel structure and the possibility of more bonds per molecule. Figure 2.13 i) shows a diagram of what this hydrogel's structure might look like. Hydrogels of this type may have up to 2.5 MPa of compressive strength [25, 35]. It is important to note that the different types of tough hydrogels discussed above are only the main categories that tough hydrogels may be classified by; there are many novel tough hydrogels in the current literature. See Peak et al. for more information on this [25] or Haque et al. for a summary on specific tough hydrogels that are applicable as biomaterials [36].

2.3.6 Fiber and Bilayer Hydrogels

Over the past ten years, researchers have examined the effect of fibers and bilayers may have on deformation and strength of material for hydrogels. The difficulty with embedding fibers in hydrogels is that they are hard to align; most research on fibers in hydrogels therefore has focused on a random orientation. Cellulose nanofibers and nanocrystals and their effects in a polyvinyl alcohol-borax hydrogel were examined by Han et al., [37]. Cellulose nanofibers from bleached wood pulp of approximate length 732nm were randomly distributed throughout the hydrogel and the rhealogical properties as compared to other hydrogels with cellulose nanocrystals were studied [37].

One interesting lamellar bilayer hydrogel is inspired by the alternating rigid and soft layers seen in shell and nacre [38, 39]. It is made of dodecylglyceryl itaconate (DGI) monomer stacked hydrophobic rigid layers that were then oriented by shear flow when immersed in a hydrophilic PAAm solution [38]. The DGI layers formed non-covalent

reversible bonds with the soft PAAm layers that served as energy dissipation mechanisms. The resulting hydrogel has anisotropic deformation when swollen; it deformed only in the direction perpendicular to the layers. Tensile tests in the direction parallel to the layers were conducted for forces up to 600 kPa. The hydrogel exhibited color change, seen below in Figure 2.14, as external forces were applied and released as well as self-recovery properties [38, 39].

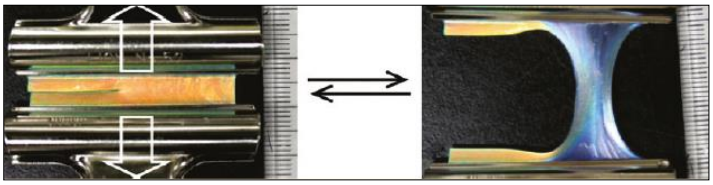

Figure 2.14 Color Change Exhibited by a DGI-PAAm Lamellar Bilayer Hydrogel in Response to an External Tensile Force [39]

In a 2012 article by Haque et al., the researchers detail many tough hydrogels and their applications as biomaterials. Two double network hydrogels of interest are made of gelatin or PAAm and combined with natural bacterial cellulose (BC) which has hydrophobic fiber networks embedded in the BC as stratified layers. As a result of the fiber network layers, anisotropic deformation was demonstrated as the gel swelled more in the direction perpendicular to the layers and very little in the direction parallel to the layers. The gelatin-BC DN hydrogel stress strain curves reveal a tensile engineering stress of over 2.5 MPa in the direction parallel to the stratified layer of the fiber network and an engineering compressive stress of over 3.5 MPa in the direction perpendicular to the stratification. Both of these values were greater than those seen in the individual gelatin and BC hydrogels [36, 40].

Fiber networks have also been put into hydrogels using rapid prototyping techniques and tools [41]. Agrawal et al. discusses the addition of elastic fibers to hydrogel in order to make them similar to natural tissues like cartilage. The fibers were made of Poly[4,40-methylenebis(phenyl isocyanate)-alt-1,4-butanediol/di(propyleneglycol)/polycaprolactone] and Texin DP7-1205 aromatic thermoplastic Urethane. The layers had fibers running perpendicular to each other in two directions and were then stacked in an epoxy-amine (polyethylene glycol diglycidylether of MW 526 and polyoxyalkyleneamines of MW 2000 or 600) hydrogel solution. Engineering stresses of over 1.8 MPa were achieved, when tensile tests were performed parallel to the direction of the fiber layers [41].

Of final note, researchers have also managed to make hydrogel fibers with an internal alignment of polymer chains through electrospinning and electrostretching. The hydrogels used were alginate, fibrin, gelatin, hyaluronic acid, and combinations of the previous. The polymer chains inside the fibers were aligned through electrospinning and then cross-linking occurred as the fiber spun to fix the polymer chain alignment in place. Fibers of fairly uniform diameter and any length were able to be made using this method and the fibers were also able to be bundled together. Mechanical properties were highly improved when tensile tested in the direction parallel to the fibers; for example, a dry fiber of calcium alginate had a Young's modulus of 10.0 GPa and a wet fiber had a Young's modulus of 717 kPa [42].

2.3.7 Stimuli Responsive Hydrogels

Hydrogels have also been synthesized to be stimuli-sensitive. A stimuli-sensitive polymer is defined by Messing et al. as undergoing "a reversible change with respect to

their conformation or phase behavior to a variation in one of the environmental parameters;" in other words, the hydrogel responds to a change in its environment by changing its shape or phase. The response of the hydrogel must be nonlinear and sudden to make it a significant response. So far hydrogels have responded to changes in temperature, pH, ions, chemicals, light, and electric fields; some hydrogels may combine a variety of these responses [43].

Hydrogels that respond to temperature are termed thermo-responsive. These hydrogels usually have a high number of hydrogen bonds per polymer and, because of this, hold a lot of water. When the gel is heated above a certain temperature (called cloud point temperature), the hydrogen bonds disappear, causing water to leave the gel and the gel to de-swell on a macroscopic scale [43, 44]. These gels are typically made of polymers containing both hydrophobic and hydrophilic groups. A thermoresponsive gel that follows the pattern of being swollen at temperatures lower than cloud point temperature and collapses at temperature above cloud point temperature is categorized as a lower critical solution temperature (LCST) type. A few hydrogels have also been made that display the opposite response; these hydrogels are termed an upper critical solution temperature (UCST) type [43].

Hydrogels that are pH or ion responsive are generally made of polymers with acidic or basic groups. A change in a pH level in the environment solution will trigger these groups to either discharge or receive protons. This results in a modification of the swollen state of the hydrogel due to electrostatic interactions that occur both between and within polymer chains [43].

Light responsive hydrogels typically respond to light due to photoisomerization or photocleavage groups that have been incorporated into the hydrogel either as pendant groups on the polymers or even cross-linking molecules [43, 44]. Photoisomerization occurs when no chemical bonds are broken but the shape and location of the bonds may change to form a different isomer of the chemical in response to light [43, 44, 45]. Photocleavage groups may be used to make photodegrable hydrogels as the photocleavage groups leave the polymers they are attached to when exposed to light. These photoisomerization and photocleavage groups may require a very specific wavelength or intensity, allowing for a fine degree of control temporally and spatially [43, 44].

Hydrogels that respond to electric fields typically have a pH gradient. The hydrogels may bend or de-swell depending on how the gel is oriented with respect to the electrodes. A variety of control methods may be exerted upon the hydrogel, including the amount of current as well as the timing of pulses and their length [43].

The responses of hydrogels to stimuli vary. Common effects are swelling and de-swelling. Some responses may be as extreme as to force the hydrogel to go from a gel back to a solution; this response is typically called a reversible sol-gel transition. In addition, permeability of the hydrogel may change [43].

2.3.8 Actuator Hydrogels

Hydrogels have been used in limited capacity to create biomimetic actuators. Hydrogel biomimetic actuators based on plant movement principles are especially rare. Sidorenko et al. investigated a device that could be considered to be plant biomimetic in its actuation. It consisted of silicon nanocolumns and two hydrogels; a polyacrylamide

gel (abbreviated PAAm) and a polyglycidyl methacrylate gel (abbreviated PGMA) [46]. The PGMA served almost as a bridge to bond with both the PAAm, which made up the body of the actuator, and the silicon wafer, which formed the base of the actuator. The research looked at two cases, seen below in Figure 2.15.

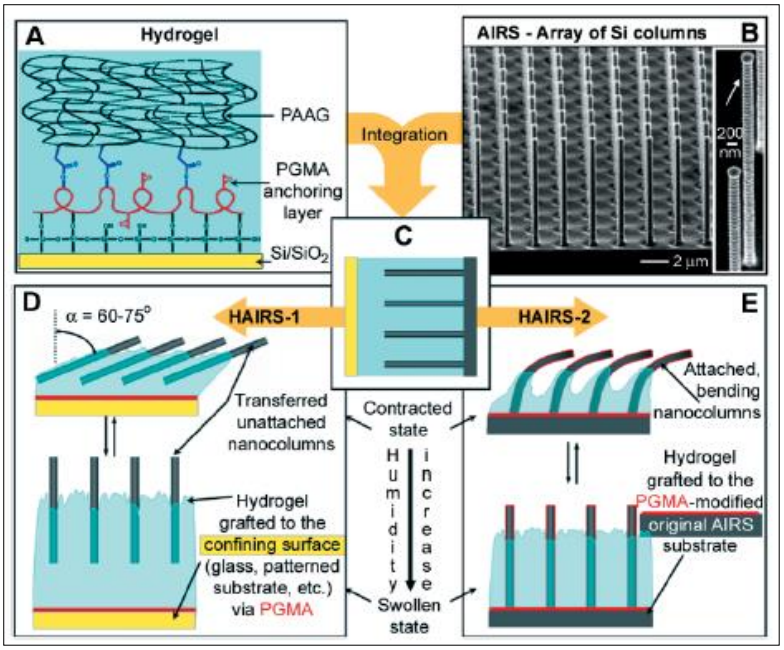

Figure 2.15 Diagram of HAIRS (A) PGMA acting as a bridge to bond to both the silicon wafer and the PAAG (B) Silicon nanocolumns and wafer base without hydrogels, termed AIRS (C) Assembled actuator with hydrogel and AIRS (d) HAIRS-1, which consists of silicon nanocolumns that have been separated from the silicon wafer; the top diagram being when the hydrogel is dry (D) HAIRS-2, which consists of nanocolumns still attached to the silicon wafer; note how the columns bend instead of rotate when in the dry state as compared to HAIRS-1 [46]

The silicon nanocolumns are manufactured on a silicon wafer, seen in Figure 2.15 (B); this arrangement was called the high-aspect-ratio rigid structure (abbreviated AIRS). The hydrogel was then sandwiched between a glass slide and the AIRS, as diagramed in

Figure 2.15 (C), and called a hydrogel high-aspect-ratio rigid structure (abbreviated HAIRS). If a HAIRS-1 case was desired, the nanocolumns were broken off of the silicon wafer and the wafer was removed, leaving unattached nanocolumns suspended in a hydrogel, as seen in Figure 2.15 (D). The top illustration of Figure 2.15 (D) shows the actuator in its contracted state, which has resulted in the nanocolumns rotating by 60-75° of their original perpendicular state when the hydrogel was swollen, seen in the bottom illustration of Figure 2.15 (D). These nanocolumns experience both tensile and compressive forces. The only cause of the change between swollen and contracted state of the hydrogel was the change in humidity. The HAIRS-2 design shows the nanocolumns still attached to the silicon wafer. In this case, they experience a bending force in the hydrogel contracted state, instead of a simple rotation due to tensile and compressive forces like seen in HAIRS-1. Once again, the biomimetic actuator reacts only to changes in humidity in its environment. It is important to consider the importance of the deformation energy that is stored in the nanocolumns in its bent state and the role of the aspect ratio in the bending of the nanocolumns and the ultimate fracture stress of the material of the wafer base. The researchers had response times of around 60 ms for the HAIRS-1; this was the time it took a fully dry HAIR to switch to a fully swollen state as the result of a water droplet being placed on its surface. The opposite process, switching from the swollen to dry state, took considerably longer with a time of around 4 seconds. The response time of HAIRS-1 did not appear to change with the number of cycles or the age of the HAIRS-1 unit. The researchers were also able to make patterns with the two different HAIRS designs, as seen in the SEM and optical images in Figure 2.16 on the next page [46].

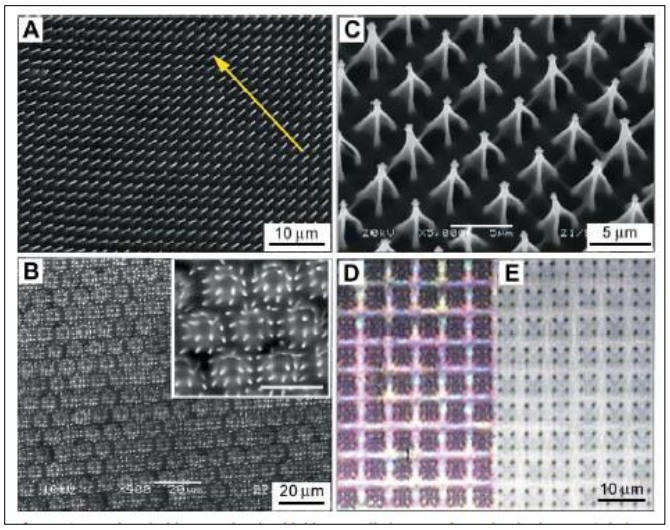

Figure 2.16 Complex micropatterns (A) Uniform pattern formed by HAIRS-1 in contracted state when parallel lines have been etched on the constraining surface in the direction of the yellow arrow (B) Contracted "mircofloret" pattern formed by HAIRS-1 as a result of a honeycomb pattern on the substrate (C) HAIRS-2 contracted "microtrap" pattern formed where "microtrap" is made up of four nanocolumns (D) The same HAIRS-1 "microfloret" pattern in swollen state (E) The same HAIRS-2 "microtrap" pattern in swollen state [46]

The contracted state of the HAIRS-1 had a random, multiple orientations of the nanocolumns, believed to be due to hydrogel thickness variations. Researchers managed to control the orientation and direction of the nanocolumns simply by patterning the confining surface or the hydrogel itself; in Figure 2.16 (A), we see the effect that a series of lines parallel to the yellow arrow patterned onto the surface. The result of parallel lines patterned onto the surface was that the nanocolumns all deformed in the same direction when in a contracted state. Figure 2.16 (B) is also made with a contraction of HAIRS-1 and is the result of a honeycomb pattern on the constraining surface; this pattern is called

"microflorets" by the researchers. Figure 2.16 (D) is a picture of the same "microfloret" pattern in the swollen state. Figure 2.16 (C) is a pattern formed by the HAIRS-2 when in a contracted state; this pattern is termed "microtraps." Figure 2.16 (E) shows the "microtrap" pattern in its swollen state. The fact that these patterns are reversible based on environmental conditions is critical to their possible biomimetic applications, such as nourishment, protection, and anti-fouling [46]. It does not appear that the researcher ever tried to scale up their hydrogel biomimetic actuator. He et al. did further research on the HAIRS, finding that the direction of actuation could also be controlled by using rectangular microfins instead of cylinders and described various ways to modify the structure to mass produce through a mold, tilt or deform the pins, and gradient shapes [47]. The researchers in this case took HAIRS-2 and evolved it into a "self-regulated mechanochemical adaptively reconfigurable tunable" (abbreviated SMART) system, seen in Figure 2.17 below.

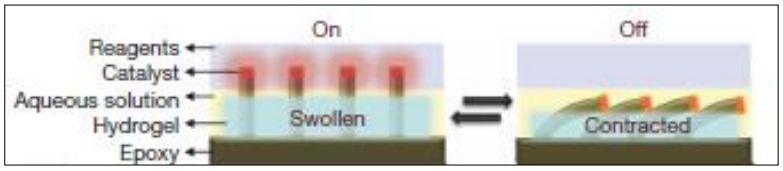

Figure 2.17 SMART System featuring a self regulating feedback loop that can convert chemical energy to mechanical energy and vice versa [47]

The SMART system features a bilayer system that consists of a hydrogel layer that will switch the microfins, whose tips are coated in catalyst, in and out of a reactant layer. The hydrogel may respond to changes in the aqueous solution that makes up the bottom layer or changes in the reactant layer; for example, the researchers propose a temperature

sensitive hydrogel that reacts to changes in the aqueous solution or to temperature change in the reactant layer caused by the chemical reactions between the catalyst and reagents. The researchers see their SMART unit as highly "tunable" to various situations and needs [47].

Besides the HAIRS and SMART actuators, some other hydrogel actuators that exist have been detailed in the paper by Maeda et al. [48]. The authors here describe two different hydrogel actuators, both operating on a cyclic chemical reaction known as the Belouzov-Zhabotinsky (BZ) reaction; the first one, termed by the authors to be a "self-walking gel," is detailed on the next page in Figure 2.18 (A). The actuators were placed on a ratcheted surface in an aqueous solution containing the BZ reactants; the ratcheted surface prevents the actuators from sliding back when they expand. The metal catalyst for the BZ reaction is bonded to the polymer chains in the hydrogel and as the BZ reaction occurs, the metal catalyst causes a change in the solubility of the hydrogel, resulting in swelling and shrinking of the gel as the chemical wave moves through it. This causes the gel to displace, seen in picture 4 in Figure 2.18 (A), and the ratchet system keeps the movement in a forward direction as the gel returns to its original c-shape after the reaction through bending. Using this gel actuator, the researchers saw a maximum velocity of 170 μm/min [48].

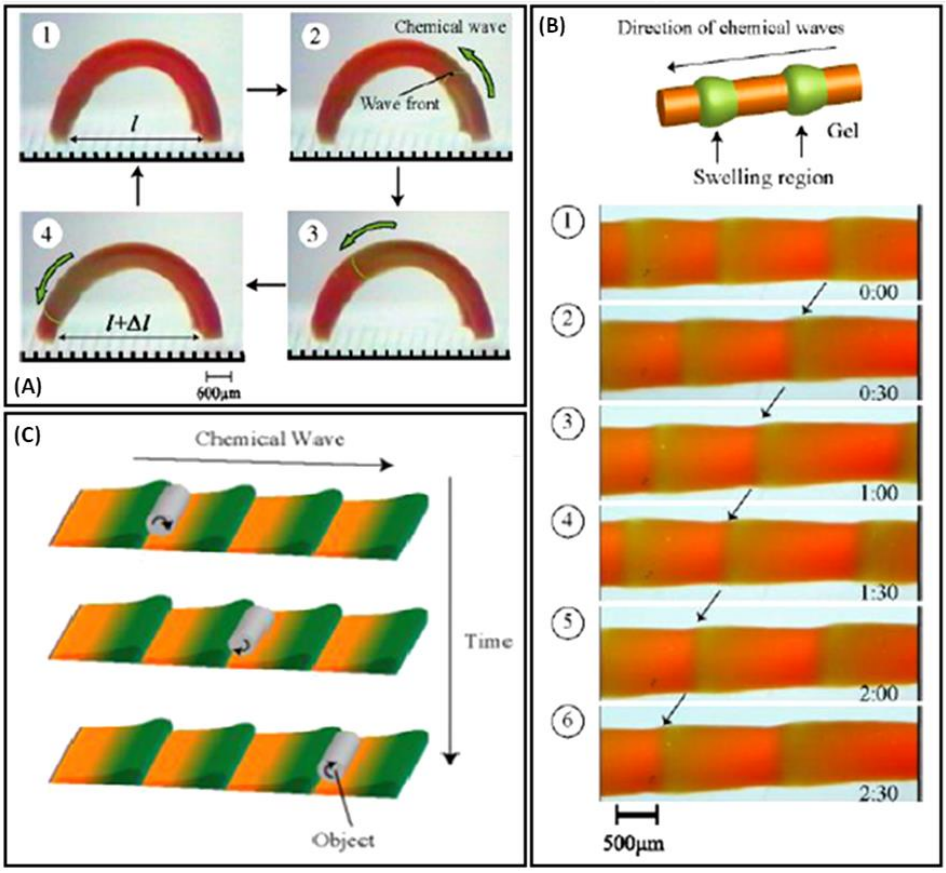

Figure 2.18 Autonomous gel actuators driven by chemical energy from the Belouzov-Zhabotinsky reaction on a ratchet surface (A) Self-walking gel with gradient structure allowing for a large deformation when the chemical wave passes through (B) Hydrogel actuator featuring "peristaltic motion" (C) Peristaltic hydrogel actuator used to transport an object [48]

The second type of hydrogel actuator discussed by Maeda et al. also uses the BZ reaction and is seen in Figure 2.18 (B) above [48]. This actuator is said to use "peristaltic motion," which is generally defined as the fluid transport caused by the expansion and contraction of areas along a cylinder containing a fluid or mixture and is taken from the term peristalsis [48, 49, 50]. The actuator was once again placed in an aqueous solution containing the BZ reactants and experience chemical waves that resulted in swelling in certain regions, which resulted in an overall forward motion when placed on the ratchet

floor. A maximum of velocity of 30 μm/s was achieved by this actuator. The authors also used this peristaltic gel to transport matter; the schematic in Figure 2.18 (C) diagrams this. A chemical wave would travel through the gel, resulting in a high degree of swelling in the green regions, which then pushed the object in the wave direction. The object had an average velocity of 40 μm/s [48].

2.3.8 Transpiration in Hydrogels

In addition to being able to actuate, hydrogels have also been used to mimic the cohesion-tension theory of transpiration in a tree by Wheeler et al. [51]. This "synthetic tree" consisted of a roof and leaf membrane and a xylem capillary that connected with them and was filled with liquid. The hydrogel used was a poly(hydroxyethyl methacrylate), also known as pHEMA, that was chemically cross-linked through photo-initiation. Liquid-filled voids were created within the hydrogel by partially setting the gel under a UV light, then placing it in a vortexer to create bubbles, and then fully setting the hydrogel in a jig with UV light. Both the leaf membrane and the root membrane contained 80 parallel channels arranged to form a circle, seen on the next page in Figure 2.19; the xylem capillary is labeled as the trunk. All microchannels were made by soft lithography.

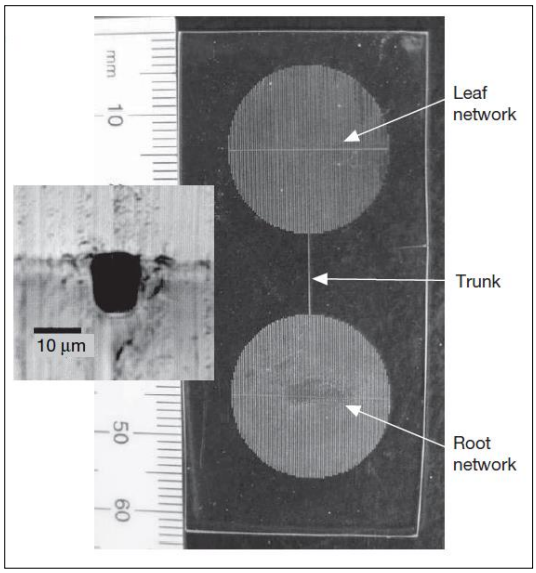

Figure 2.19 Picture of Synthetic Tree on pHEMA featuring a leaf and root section with a xylem capillary trunk connecting them. The inset shows the microchannels created through soft lithography [51]

The pressure difference between the root network and the leaf network is what drives transpiration as water molecules evaporate in the leaf network due to air flow across it, pulling water up the trunk behind it through the tension-cohesion theory. The researchers did have some problems the tensile force created by the water not being strong enough due to the formation of vapor which led to cavitations. They believed the cavitations were the consequence of temperature resulting in phase change; not the surrounding air crossing the membrane boundary or pre-existing nuclei expansion [51].

2.3.9 Rapid Prototyping of Hydrogels

Hydrogels have also been manufactured using rapid prototyping methods; the biggest driver in this area of research is the idea of using hydrogels as scaffolds for tissue

engineering applications. Billiet et al. looked at the current trends and constraints in the rapid prototyping of hydrogel scaffolds for hard and soft tissue regeneration and categorized them by manufacturing system type; laser-based, nozzle-based, and printer-based [19]. Scaffolds allow for a set porosity and geometry [19].

Laser-based engineering involves using a photopolymerizable polymer in a solution and using light energy to pattern it into a hydrogel scaffold. The main types of laser-based rapid prototyping are all suitable for hydrogels with the exception of laser sintering; this includes techniques such as stereolithography (SLA), micro-stereolithography (μ-SLA), solid ground curing (SGC), and two photon-polymerization (2PP). Stereolithography features a liquid reservoir of photopolymerizable precursor hydrogel solution in which a fabrication platform is immersed. The fabrication platform is what the specimen is built on and allows for movement in the vertical (often called Z) direction. The hydrogel specimen is polymerized by a laser, which commonly has an ultraviolent (UV) spectrum, and the direction of this laser beam is controlled in the horizontal (often called the X-Y) direction by some type of scanner system. SLA and μ-SLA are the same technique; the only difference is scale with μ-SLA being on the order of microns. SLA and μ-SLA are really a layer-based approach with 2D patterns being laid out by the scanner system and laser and then the fabrication platform adjusting in the Z direction to build the next layer. This method may use a top down or bottom up fabrication approach; in a top down SLA setup, the laser and scanner system are located above the liquid reservoir and the specimen sits on top of the fabrication platform. In the bottom up SLA layout, the laser and scanner system are below the liquid reservoir and the specimen sit below the fabrication platform. Obviously the container holding the

liquid reservoir must permeable laser light so that it can reach the photopolymerizable solution. It is also important to note that often these specimens must be further cured after being removed from the liquid reservoir. One area of interest in SLA and μ-SLA is digital light projection (often seen as DLP in literature), which allows for the curing of one layer in a single instant of exposure to a laser; frequently this is done through a system of mirrors that can turned into an on or off position depending on the pattern of the layer being polymerized [19].

SGC features a layer by layer approach as well with a fabrication platform. In this case however, there is no movement by the platform or the laser/scanner system in the X, Y, or Z direction. Instead, a thin layer of the photopolymerizable precursor solution is laid down on the fabrication platform and a photomask specific to this layer is made by the machine and placed above the fabrication platform. The fabrication platform is then exposed to light and the thin layer of precursor solution is cured. Excess solution is then removed, wax is added to fill in any holes in the pattern so that it can support the next layer, and the layer that has just been fabricated is milled flat to get rid of any inconsistencies. The platform is then sprayed again with the photopolymerizable solution, a new photomask is created, and the entire process is repeated again [19].

2PP uses a photopolymerizable solution reservoir and two lasers. The two lasers, with wavelength of 800nm and impulse on the order of femtoseconds, meet at a focal point in the solution where the polymerization into a hydrogel is to take place. Two photons are donated from each laser simultaneously and absorbed by the photoinitiator acting as a single photon of 400nm. This technique is highly accurate and polymerization occurs only at the focal point, leaving the surrounding solution completely impervious. The

technique can truly work in 3D, as opposed to a layer by layer technique seen in SLA, µ-SLA, and SGC, and features of less than 100nm have been able to be accurately produced on micron-sized objects [19].

Nozzle-based hydrogel rapid prototyping has a wide variety of techniques; most of the common techniques involve raising the temperature of the material so that it melts, which is usually unsuitable for tissue engineering hydrogel scaffolds that involve biomaterials or cells. Researchers have found a way around this by developing specialized nozzles such as pressure-assisted microsyringe (PAM), low-temperature deposition modeling (LDM), 3D-Bioplotter system, rapid prototyping robotic dispensing (RPBOD) system, robocasting, direct ink writing (DIW), and extruding/aspiration patterning system. All of these techniques are manufactured layer by layer. PAM uses an air-driven glass syringe and a substrate platform. The substrate platform moves in the horizontal direction and the syringe moves in the vertical direction [19].

LDM features a method that doesn't use heat to liquefy materials as they are processed. A nozzle moves in the horizontal direction to deposit the liquid that then solidifies on a fabrication platform that move in the vertical direction at temperature below 0°C. This method has also proposed using multiple nozzles and is then abbreviated either as MDM or M-LDM [19].

In a 3D-Bioplotter system, the dispensing head may move both horizontally and vertically and it deposits material, either as a continuous strand or as dots, onto a stationary fabrication platform by layers. It operates on the order of microns and can operate using either a pneumatic or volume driven injection nozzle. Strand thickness may be controlled through a variety of factors. This method can dispense into a liquid media

as long as densities match and can have more than one nozzle. RPBOD is analogous to the 3D-Bioplotter system and features a single pneumatic dispensing unit [19].

Robocasting features hydrogel solutions combined with a ceramic slurry that liquefy under pressure so that they can leave the dispensing head and being deposited onto a fabrication platform that moves in horizontal and vertical directions. Once deposited, the material is no longer under as much stress and hopefully recovers its stiffness and partially dries before the next layer is deposited. This method doesn't allow for pure hydrogels [19].

DIW involves colloid (which are hydrophilic polymers) gels held in syringes that are deposited through a nozzle that move in the vertical direction. The fabrication platform moves in the horizontal direction. These colloid gels must be a liquid through the nozzle and then solidify when or soon after their deposition onto the platform. The fraction of colloid per volume must be relatively high to assure that the shrinking after drying is not significant [19].

In an extruding/aspiration patterning system, the modes can easily be switched from extruding to aspiration and vice versa, allowing for an assortment of applications. It is even possible to use a thermo-reversible hydrogel. In this method, the whole fabrication process it temperature- and humidity controlled. A nozzle containing a valve deposits the material onto a substrate. When the valve connected to the nozzle is closed, compressed air forces an extrusion. When the valve connected to the nozzle is open, compressed air forces an aspiration [19].

Printer-based rapid prototyping methods specifically refer to those methods using inkjet or printer technology in this literature review. All printer-based techniques are

layer by layer and there are a wide variety of only slightly different adaptations of these technologies; therefore only the general printer-based ink jet processes will be discussed here. A good example of a general printer-based technology 3D Printing (3DP^{TM}) technology, which features a reservoir of powder and a reservoir containing the fabrication platform. A roller takes polymer powder from the reservoir and rolls it over the fabrication platform (which moves in the vertical direction) and then a liquid binder dispenses from an inkjet print head above the platform and solidifies the pattern as it moves in the horizontal direction. These steps are repeated until the 3D object is achieved. There are limits on the size of the smallest features that can be places on objects and limits on the object dimensions and these are governed mostly by the interactions that occur between the binder and the powder particles. Printer based technologies may also use hydrogel solution reservoirs in place of the powder reservoir that still transfers the solution to the fabrication platform using a roller or they may directly dispense the hydrogel solution from the ink jet printer head [19].

Rapid prototyping of hydrogel allows for complex shapes of hydrogels. Hydrogels with complex shapes, such as shapes outside of rectangle and cylinders, could enable the production complex actuators. In the future, these complex shapes could possibly be imbued with fibers (from another nozzle perhaps) aligned in specific directions to allow for plant biomimetic actuators.

2.3.10 Applications of Hydrogel Actuators

Hydrogels have been suggested for many applications; most of them are biomedical in nature due to some hydrogels' biocompatibility. The possibility of using hydrogels for artificial muscles has been proposed since the basic principles of muscle

movement rely on fast, reversible, shortening and lengthening in one direction. Many researchers focus on creating a version of cartilage with hydrogels [43]. Cartilage, cornea, dermis, and arterial walls are all fiber-reinforced gels and cartilage and cornea in particular need synthetic substitutes [24]. Hydrogel actuated microvalves could also be made; especially with a stimuli-responsive hydrogel, where the stimulus could be in the flow or external to it [24, 43]. Actuators could also be applied as sensors that respond to environmental stimuli through volume or shape change as well as a change in their properties, such as resistivity or color [24].

Chapter 3 – MATERIALS AND METHODS

3.1 CHEMICALS

Polyethylene glycol diacrylate (abbreviated PEG-DA, MW 575, product #437441) and 2-hydoxy-2-methylpropiophenone (MW 164.2, product #405655) were purchased from Sigma-Aldrich Chemical Company (Milwaukee, WI) and stored in a refrigerator along with deionized water. Silicone glass adhesive (DAP® All-Purpose Adhesive Sealant UPC #70798 00688) was used for parts of the mold.

3.2 METHODS

Note that gloves made of nitrile rubber were worn for all procedures. Also, all hydrogel solutions vary only by the photoinitiator [v/v] %; the amount of PEG-DA in the solution is always a constant 20% [v/v]. Thus a 1% PEG-DA hydrogel really means 1% photoinitiator, 20% PEG-DA and a 0.1% PEG-DA hydrogel means 0.1% photoinitiator, 20% PEG-DA.

3.2.1 Single Layers

1% Layer:

20% [v/v] PEG-DA was reverse pipetted into a 1.5mL Eppendorf tube. Then 79% [v/v] deionized water and 1% [v/v] of the photoinitiator, 2-hydroxy-2-methylpropiophenone, were added to the PEG-DA. The mixture was vortexed for five minutes. The solution was pipetted into a glass mold that made a sample that was approximately 25 x 13 x 2.4 mm and was held together by a combination of silicone

adhesive holding the frame together and 1% PEG-DA hydrogel (1% photoinitiator, 20% PEG-DA) adhering the frame to the glass slide used as a base. A glass top was then placed on top of the mold and the solution was exposed to a UV lamp (Blak-Ray® B-100YP Model, 365nm wavelength, 100W power) placed approximately 20 cm directly above the sample for eight minutes. The hydrogel were then removed from the mold and allowed to soak in deionized water for at least 12 hours to remove any unreacted solution.

0.1% Layer:

The same methods were used for the 0.1% layer; the only differences were that 0.1% of photoinitiator and 79.9% [v/v] deionized water were added to the Eppendorf tube. Briefly, 20% [v/v] PEG-DA,79.9% [v/v] deionized water, and 0.1% [v/v] of the photoinitiator were added together and vortexed for five minutes before being pipetted into the 25 x 13 x 2.4 mm mold and covered by a glass top. The mold was exposed to a UV lamp for eight minutes, removed, and allowed to soak in deionized water for at least 12 hours to remove any unreacted solution.

3.2.2 Bilayers

1%-0.1% Bilayer

The solution was made according to the methods previously laid out for the 1% layer (1% [v/v] photoinitiator, 20% [v/v] PEG-DA, and 79% [v/v] deionized water, vortexed together for five minutes). The solution was then pipetted into a glass mold that made a sample that was approximately 25 x 13 x 1.2 mm, held together by the 1% PEG-DA hydrogel (1% photoinitiator, 20% PEG-DA). A glass top was then placed on top of the mold and the solution was exposed to a UV lamp for eight minutes. The top was then removed from the mold and another glass mold of the same size (25 x 13 x 1.2 mm) was

adhered on top of the current mold using 0.1% PEG-DA hydrogel solution (0.1% photoinitiator, 20% PEG-DA) and set with UV lamp exposure of approximately 2 minutes. A solution was then made according to the directions previously listed in the 0.1% layer (0.1% [v/v] photoinitiator, 20% [v/v] PEG-DA, and 79.9% [v/v] deionized water, vortexed together for five minutes). This solution was then pipetted into the mold over the 1% hydrogel sample and a top was laid across it before it was exposed to UV light for eight minutes. The hydrogel bilayer was then removed from the mold and allowed to soak in deionized water for at least 12 hours to remove any remaining unreacted solution.

3.2.3 Random Orientation Fiber Bilayer

Fibers, colloquially known as "chop," were placed in a glass mold (adhered together with 1% PEG-DA hydrogel) that produced a sample size of 25mm x 13mm x 1.2mm and spread out until they appeared evenly distributed. A solution of 1% PEG-DA hydrogel (1% photoinitiator, 20% PEG-DA) was then made and pipetted into the mold. The fibers were once again adjusted to make sure that they appeared to be evenly distributed and then a glass top was placed on the mold and the solution was exposed to UV light for eight minutes. The top was then removed, and another glass mold of the same size (25mm x 13mm x 1.2mm) was adhered in place with 1% PEG-DA hydrogel solution and set through a UV exposure of approximately two minutes. A solution of 1% PEG-DA hydrogel was then pipetted into the mold on top of the random distribution fiber layer and a glass cover was placed on top and the mold was exposed to UV light for another eight minutes. The sample was then removed from the mold and allowed to soak in deionized water for a minimum of 12 hours to remove unreacted solution.

3.2.4 Perpendicular Alignment Glass Fiber Bilayer

Glass fibers of approximately 80mm length were taken and aligned by holding one end of a group of fibers down with a gloved finger on a piece of paper and essentially brushing the fibers to align them with the other gloved finger. The fibers were spread out evenly and then held down on the opposite end and brushed the other way as well until a uniform distribution appeared to be reached. The base of the mold, which was just a typical glass microscope slide (25 x 75 x 1.2 mm) was then wetted around both 25 mm edges with approximately 30μL of 1% PEG-DA hydrogel solution each and placed face down onto the glass fibers so that the length of the fibers were parallel with the 75mm edge of the slide. The slide and paper together were carefully flipped over and then the paper was gently peeled away from the slide. Any issues with fiber alignment were then carefully fixed with tweezers. A 1% PEG-DA solution was then placed onto the bottom of a glass frame held together with silicone adhesive of sample size 25 x 13 x 2.4 mm. The mold was then set under UV exposure of approximately two minutes to make sure the base slide adhered to the glass frame. Another group of glass fibers was taken and aligned as described previously. This time the fibers were taped down on both ends onto the paper. The top of the mold was then wetted along the 75mm sides with 1% PEG-DA solution and one side of the taped fibers was carefully peeled up. The mold was slid under the fibers so that they were perpendicular with the previous layer (in other words, the fibers ran parallel to the 25mm side of the glass slide) and the tape was then stuck back onto the sheet of paper. Any fiber alignment issues were fixed with tweezers and then a solution of 1% PEG-DA hydrogel was pipetted into the mold and carefully covered with a glass top. The sample was exposed to the UV lamp for eight minutes and

then removed from the mold and allowed to soak for at least 12 hours to remove any unreacted solution.

3.2.4 Testing

The displacement of the layers and bilayers was tested by taking soaked hydrogels and hanging them using a needle and thread to poke a hole approximately a third of the way down from the top of the hydrogel. This method was used because it was important to constrain the hydrogel by as little as possible as it was noticed that the method by which the hydrogels were constrained greatly affected their deformation.

Chapter 4 – RESULTS

4.1 CONTROLS AND 1%-0.1% BILAYERS

The hydrogel specimens usually took a little over 12 hours to dry completely. The control single layers of 1% and 0.1% did display some curvature during the drying process due to the fact that drying occurred at the edges of the layer first, which resulted in shrinking at the edges and not the middle thus leading to deformation. However, once dried, these specimens retained a roughly rectangular shape with no significant bending. Figure 4.1 below shows the 1% and 0.1% control layers before the drying process started, the curvature seen in the middle of the drying process, and the shape of the hydrogel after the drying process.

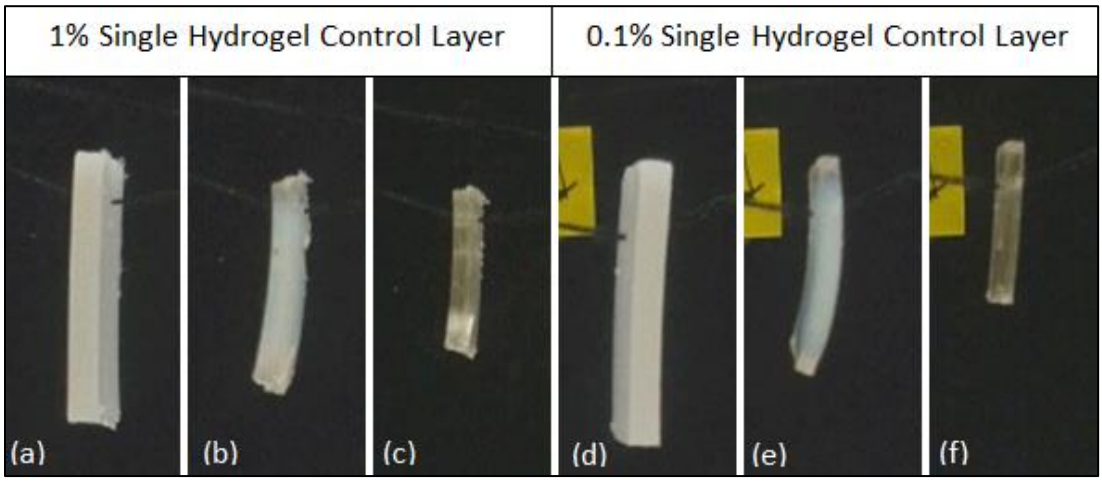

Figure 4.1 1% and 0.1% Control Layers and the curvature seen during drying (a) 1% single layer used as a control before drying (b) 1% single layer curvature seen in the process of drying (c) 1% single layer after drying over 12 hours (d) 0.1% single layer used as a control before drying (e) 0.1% single layer curvature seen in the process of drying (f) 1% single layer after drying over 12 hours

Eight specimens of the 1%-0.1% Bilayer were examined; these specimens are labeled A through G. The 1%-0.1% bilayers were more unpredictable than the fiber bilayers, which will be discussed later. Specimen A is pictured below in Figure 4.2; the 0.1% layer is on the left side and the 1% layer is on the right side of the specimen. Even though splitting and cracking occurred, the specimen still ended up bending towards the 0.1% layer, seen in Figure 4.2 (c).

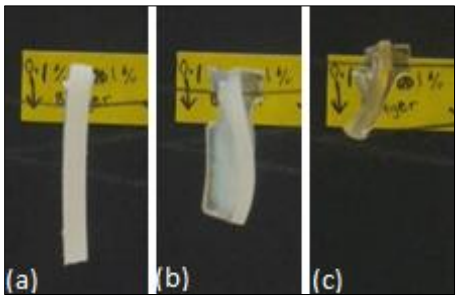

Figure 4.2 Specimen A of 1%-0.1% Hydrogel Bilayer with 0.1% on the left and 1% on the right of the bilayer (a) Freshly removed from soaking (b) Exhibiting typical curvature seen in the hydrogel drying process (c) After drying over 12 hours

Specimen B is pictured on the next page in Figure 4.3. The 1% layer is on the left and the 0.1% layer is on the right of the specimen. Once again, specimen bends towards the 0.1% layer after drying, seen in Figure (c). This was an excellent specimen that did not exhibit any cracking or splitting.

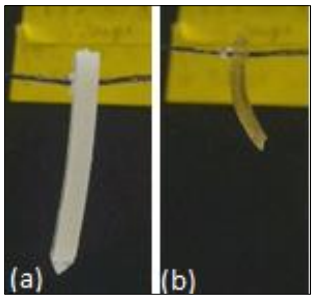

Figure 4.3 Specimen B of 1%-0.1% Hydrogel Bilayer with 1% on the left and 0.1% on the right of the bilayer (a) Before (b) After a drying period of over 12 hours

Figure 4.4 below displays specimen C before and after drying in (a) and (b) respectively. The 1% side is on the left and the 0.1% side is on the right of the hydrogel. This bilayer actually split down the middle, seen in pictures (c) and (d), but still bent towards the 0.1% side after drying.

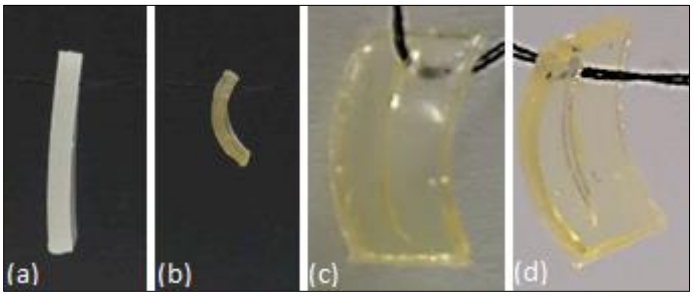

Figure 4.4 Specimen C of 1%-0.1% Hydrogel Bilayer with 1% on the left and 0.1% on the right of the bilayer (a) Before (b) After a drying period of over 12 hours (c) Cracking viewed from the 1% layer (d) Cracking viewed from the 0.1% layer

Specimen D actually ended up splitting apart during the drying process. This hydrogel is pictured below in Figure 4.5, with the 1% on the left side and the 0.1% on the right side of specimen. This hydrogel began splitting within two hours after the drying process began.

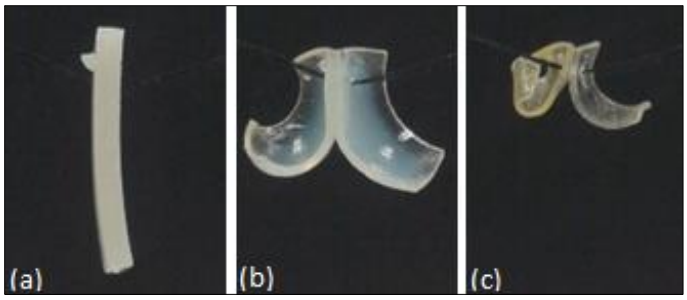

Figure 4.5 Splitting Specimen D of 1%-0.1% Hydrogel Bilayer with 1% on the left and 0.1% on the right of the bilayer (a) Before (b) After a drying period of approximately four hours (c) After approximately eight hours

Figure 4.6 on the next page shows Specimen E, which developed a crack leading from the hole with the string to the edge of the specimen approximately four hours into the drying process. The hydrogel had been curving in the right direction when it cracked horizontally, seen in Figure 4.6 (b). When the specimen was dry, it was discovered that it had cracked in numerous places and dried into a relatively straight specimen, seen in Figure 4.6 (c) and (e).

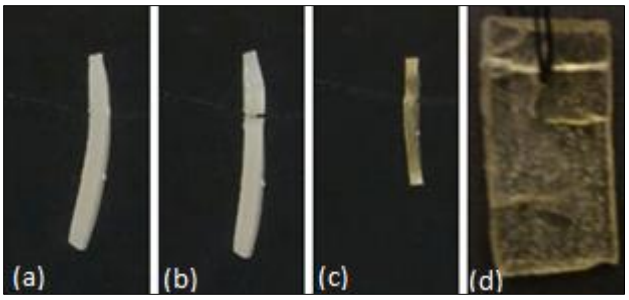

Figure 4.6 Specimen E of 1%-0.1% Hydrogel Bilayer with 0.1% on the left and 1% on the right of the bilayer (a) Right before cracking occurred (b) 10 minutes later (d) Dry hydrogel (e) Numerous cracks in the dry hydrogel

Specimen F below exhibited curvature around the shorter axis of the hydrogel instead of the long axis, as seen in Figure 4.7 (a). The shorter axis bent towards the 0.1% layer. There was no apparent cracking in this sample.

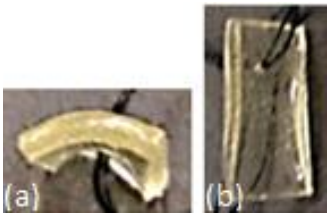

Figure 4.7 Specimen F of 1%-0.1% Hydrogel Bilayer (a) Curvature occurred on long the shorter axis instead of the long axis of the hydrogel (0.1% layer is on the bottom and 1% layer is on the top) (b) Photo taken from the 0.1% layer side

Specimen G exhibited some curvature along the shorter axis, seen in Figure 4.8 (a) on the next page, although not as significant as seen in Specimen F. This hydrogel had

a long crack running through it that started where the string was pulled through the hydrogel and the crack was not precisely parallel with the longer side. The crack can be seen in Figure 4.8 (b).

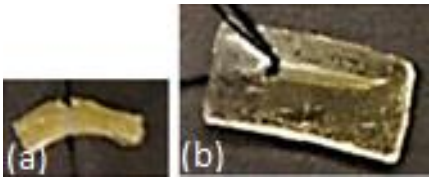

Figure 4.8 Specimen G of 1%-0.1% Hydrogel Bilayer (a) Curvature occurred on long the shorter axis instead of the long axis of the hydrogel (0.1% layer is on the bottom and 1% layer is on the top) (b) Crack in the hydrogel sample

4.2 RANDOM FIBER ORIENTATION BILAYERS

Specimen H can be seen on the next page in Figure 2.28. Figure 4.9 (a) and (b) are before and after photos of the hydrogel drying with the randomly oriented fiber layer on the left of the specimen. Curvature occurred so that the random fiber layer was on the outside of the curve. Figure 4.9 (c) shows how the bilayer curved into a circular shape and (d) shows how the bilayer actually overlapped itself in places. One side appears to have actually curled tighter than the other side.

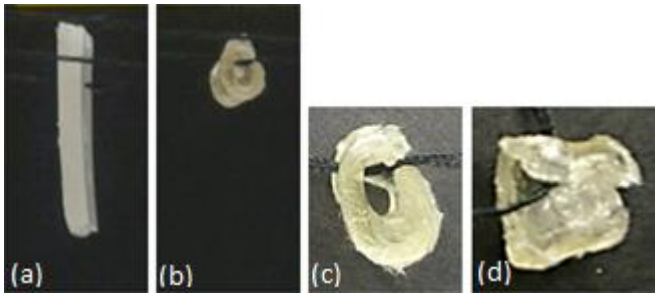

Figure 4.9 Specimen H of 1% Random Fiber Orientation Hydrogel Bilayer with fiber layer on the left (a) Before (b) After a drying period of over 12 hours (c) Dried Specimen Curved around Itself into a Circular Shape (d) Front View of Bilayer where it wraps around itself

Specimen I also wrapped around itself and displayed the same trends of having one side curled tighter than the other, seen in Figure 4.10 (c) and (d) below. Figure 4.10 (a) and (b) displays the before and after side shots of the hydrogel drying. The random orientation fiber layer was on the left of the specimen for (a) and (b) of Figure 4.10. Once again curvature occurred so that the random fiber layer on the outside of the curve.

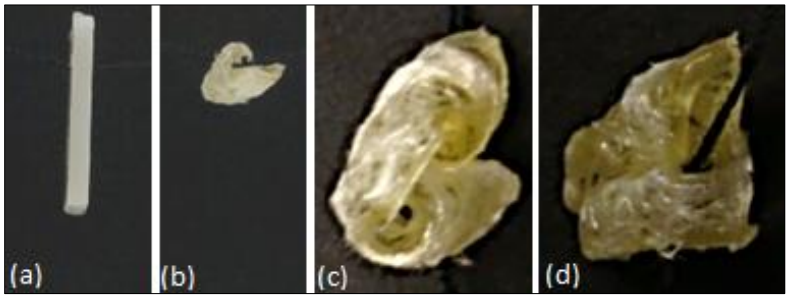

Figure 4.10 Specimen I of 1% Random Fiber Orientation Hydrogel Bilayer with fiber layer on the left (a) Before (b) After a drying period of over 12 hours (c) Side view of the hydrogel wrapping around itself (d) Front view of the specimen wrapping around itself

Figure 4.11 below shows photos of Specimen J. Figure 4.11 (a) and (b) are the side photos of the hydrogel specimen before and after drying with the random fiber layer on the left of the specimen. The curvature followed the same trend as the previous random fiber bilayers as it curved so that the random fiber layer was on the outside of the curve. Once again, as the photos in Figure 4.11 (c) and (d) show, the specimen wrapped in on itself with one side experiencing a tighter curl than the other.

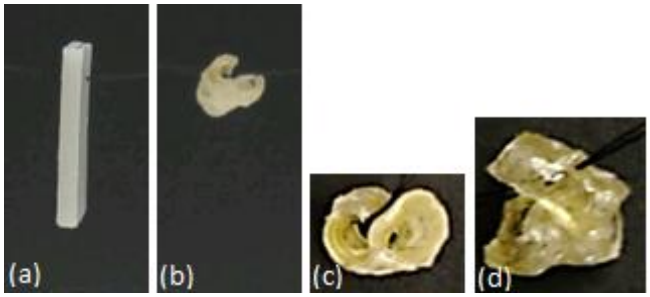

Figure 4.11 Specimen J of 1% Random Fiber Orientation Hydrogel Bilayer with fiber layer on the left (a) Before (b) After a drying period of over 12 hours (c) Side view of the hydrogel wrapping around itself (d) Front view of the specimen wrapping around itself

4.3 PERPENDICULAR FIBER BILAYERS

Before and after photos of specimen K drying can be seen in Figure 4.12 (a) and (b) on the next page; the left side of the hydrogel has fibers in the vertical direction and the right side has fibers in the horizontal direction. The sample exhibited significant curvature along the longer axis as well as the shorter axis, as can be seen in Figure 4.12 (c) and (d). Note the cracks highlighted by the red circle in (c) and that these cracks are on the right side in (d) which doesn't curve in quite as much as the left side.

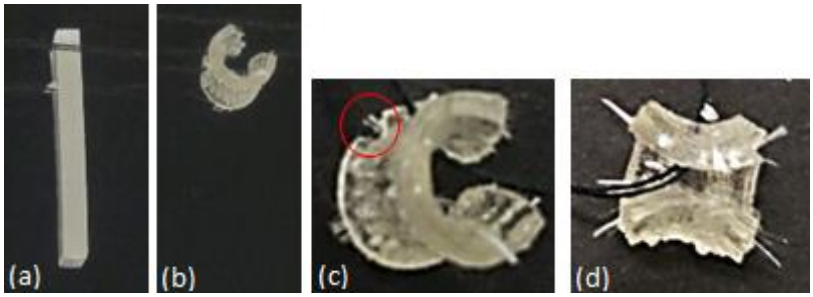

Figure 4.12 Specimen K of 1% Perpendicular Fiber Orientation Hydrogel Bilayer with vertical fiber layer on the left and horizontal fiber layer on the right (a) Before (b) After a drying period of over 12 hours (c) Side View of the Specimen after Drying (note the crack on the left side (d) Front View of Specimen Curling Towards the Camera

Photos of specimen L drying can be seen on the next page in Figure 4.13 (a) and (b). Once again, the fibers on the left of the specimen are vertical and the fibers on the right are horizontal. The sample followed the same trend as Specimen K and exhibit curvature around the long and short axes, seen in Figure 4.13 (b) and (c). Specimen L's curvature along the longer axis isn't as substantial as Specimen K's curvature along the same axis. This specimen also has less curvature along the shorter axis as seen in Figure 4.13 (c) on the right side, which could be the result of cracks, one of which can be seen in the photo circled in the red. The second crack can be seen in the side photo of the hydrogel specimen seen in Figure 4.13 (d), where both cracks are circled in red.

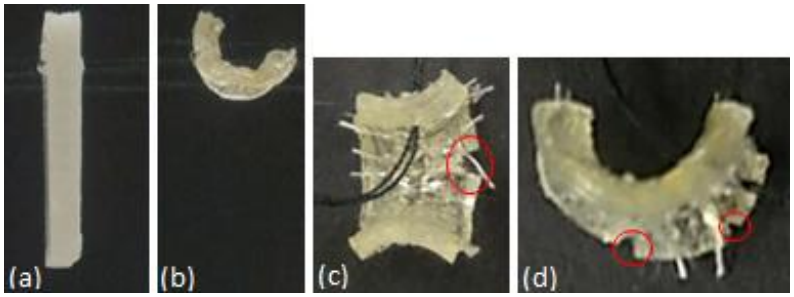

Figure 4.13 Specimen L of 1% Perpendicular Fiber Orientation Hydrogel Bilayer with vertical fiber layer on the left and horizontal fiber layer on the right (a) Before (b) After a drying period of over 12 hours (c) Front View of Hydrogel Curling Towards the Camera (d) Side view of the hydrogel

Specimen M photos may be seen on the next page in Figure 4.14; part (a) and (b) are the before and after photos of the drying process with the left side having horizontal fibers and the right side having vertical fiber layers. The specimen exhibited the same trend as previous perpendicular fiber bilayer specimens; curvature was seen along both the short and long axes. Figure 4.14 (c) has a photo of the bilayer curling towards the camera; there is a large crack on the bottom of the specimen, which doesn't curve quite as far in as the top. However, as exhibited by Figure 4.14 (d), there are cracks on both sides of the specimen.

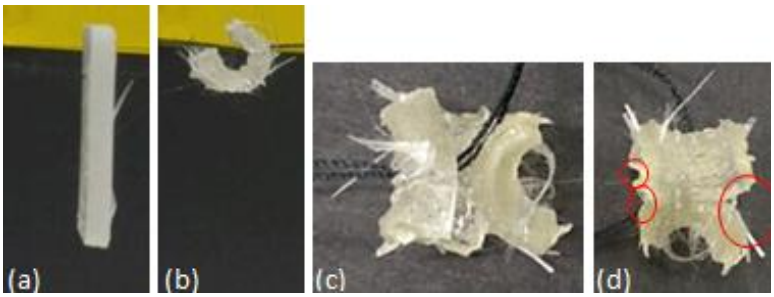

Figure 4.14 Specimen M of 1% Perpendicular Fiber Orientation Hydrogel Bilayer with horizontal fiber layer on the left and vertical fiber layer on the right (a) Before (b) After a drying period of over 12 hours (c) Front view of the hydrogel curving towards the camera (d) Back View of the hydrogel with showing other cracks that developed as well

Specimen N before and after drying photos can be seen in Figure 4.15 (a) and (b) below; the layer on the left of the specimen has vertical fibers and the layer on the right side has horizontal fibers. The sample exhibited curvature in both the long and short axes, as can be seen in Figure 4.15 (c). No significant cracks were observed.

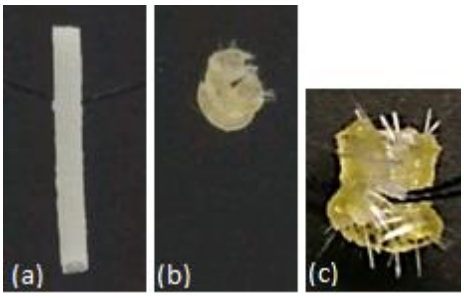

Figure 4.15 Specimen N of 1% Perpendicular Fiber Orientation Hydrogel Bilayer with vertical fiber layer on the left and horizontal fiber layer on the right (a) Before (b) After a drying period of over 12 hours (c) Front view of fiber curling towards camera

Chapter 5 – DISCUSSION

Specimens A, B, and C of the 1%-0.1% bilayers behaved as expected; the consequence of having one side more tightly cross-linked (the 1% layer) and the other more loosely cross-linked (the 0.1% layer) resulted in a different swelling abilities. The 0.1% layer could therefore swell more and shrink more than the 1% layer due to a looser cross-linked network that can fit more water molecules when swollen. This meant that when the hydrogel bilayers dried, the 0.1% layer would shrink more than the 1% layer, causing the hydrogel to bend towards the 0.1% side. This is analogous to the theory behind a bimetallic strip and the idea for this design was based on plant movement driven through unequal expansion of cells. It was expected that the bilayers would bend along the longer side and Specimens A, B, and C did this.

Specimens F and G also displayed the expected behavior of bending in the direction of the 0.1% layer but these bilayers bent along their shorter side instead of the long side as Specimen A, B, and C did. This was unexpected but it could be that the force of gravity was strong enough to oppose their movement of bending along the longer axis due to the way they were set up. It is also interesting to note that Specimen G has a crack that started at the hole where it was hung that stretches downwards approximately paralleling the longer sides of the hydrogel and Specimen G displays less curvature along the shorter axis than Specimen F, which has no visible cracks. There may be a correlation between cracking and corresponding curvature achieved.

The 1%-0.1% bilayers were the most unpredictable of all the bilayers created because they tended to have larger cracks and split a lot more when compared to fiber bilayers. Many of these 1%-0.1% bilayers cracked before they were even taken out of the mold. These bilayers were always constructed so that the 1% layer was on the bottom so that even if some of the fluid from the 0.1% layer did penetrate the 1% layer during UV radiation, the network in the 1% layer simply became even more tightly cross-linked. Also, since the 1% layer was on the bottom, this meant that any unreacted fluid in the 1% hydrogel layer would have to fight gravitational forces in order to go from the high concentration in the 1% layer to the lower concentration in the 0.1% layer while UV radiation occurred.

Cracking in these bilayers occurred in both the vertical and horizontal directions and frequently started at the hole through which the hydrogel was hung. There might be a correlation between cracking in specific locations on the hydrogel and how much curvature was achieved subsequently. Specimen D, which is the hydrogel that split apart as it dried, is interesting because it the left side, which was the 1% side, curled more once it was dry than the right side, which was 0.1% side. However, it is impossible to determine how evenly the specimen split apart; it could be that right side (the 0.1% side) still had a thin layer of 1% on it that prevented it from curling as much as it would have.

The design of the bilayers with one layer of randomly oriented fibers was loosely based on fiber actuation concepts seen in the wheat awn. Specimens H through J did not display as much smooth or uniform deformation along the short and long axes when compared to the perpendicular fiber and 1%-0.1% bilayers. The lack of smooth deformation could be due to the random fiber not being distributed uniformly enough

throughout the hydrogel layer. The random fiber bilayers did, however, display the most curvature along the longer axis. In all the specimens, it appeared that the string on which they hung may have prevented the hydrogel bilayer from curling around itself and caused one side to curl tighter than the other in order to avoid the string. These bilayers behaved as expected; the 1% layer without fibers shrunk more when compared to the 1% random fiber layer where the fibers constrained the shrinking. This meant that the bilayer curved towards the 1% side without fibers. The random fiber bilayers also did not display as many visible cracks as the 1%-0.1% bilayer and the perpendicular fiber bilayers.

The perpendicular fiber bilayers, Specimens K through N, behaved as expected as well. The fibers were expected to allow deformation (or shrinking) only in the direction perpendicular to them. This relates back to the discussion of fibers embedded in plants in Section 2.2.2, Figure 2.3 (B), which shows the deformation occurring only in the direction perpendicular to the fibers. In these bilayers, the fibers parallel to the shorter side would result in deformation occurring along the longer side; in other words the only the longer side would shrink in this layer. The fibers parallel to the longer side in the other layer were expected to have the opposite effect; they would restrict this layer so that it only experienced deformation along the shorter side. Therefore the shorter side in this layer would shrink. When the fiber layers were combined in a hydrogel so that they were perpendicular to each other, the shorter fibers in one layer allowed for shrinking only along the longer side while the longer perpendicular fibers in the other layer resisted shrinking in that direction, resulting in curvature along the longer side towards these short fibers. This same curvature was achieved along the shorter side as well due the longer fibers allowing shrinking along the short side and the shorter fibers perpendicular to them

resisting shrinking. This resulted in curvature along both the short and long axis. This is analogous to the pine cone example discussed in Section 2.2.2 and seen in Figure 2.7, except that fibers the orientation of how the fibers are perpendicular to each other has changed.

Cracks in the perpendicular fiber bilayers appeared to influence the amount of curvature achieved; this seemed to have a visible effect on the curvature in the longer axis. Hydrogels that had cracks on their long sides didn't seem to curve quite as far in along that axis. The cracks seen in the perpendicular fiber hydrogels were generally smaller in length than the cracks seen in the 1-0.1% bilayers, which might be due to an increase in overall hydrogel strength due to the fibers.

Chapter 6 – CONCLUSION

Most of the bilayers displayed the expected behavior. The 1%-0.1% bilayers generally displayed curvature towards the 0.1% layer as a result of the dissimilar shrinking rates created from the difference in cross-linking density between layers. Three of these bilayers curved along their longer axis and two curved around their shorter axis. The two remaining 1%-0.1% bilayers did not curve at all as a bilayer; this could possibly be due to the cracking or splitting that occurred. This bilayer actuation design was based on plants moving through unequal expansion of cells.

The random fiber bilayer hydrogels also displayed the predicted behavior as well; the fibers in one layer restricted shrinking rates while the other fiber-less layer shrunk at its usual rate. The result of the two different shrinking rates caused bending to occur towards the layer without fibers. The curling of the specimens along their longer axis may have been restricted by the string the bilayer was hung from; this string may have also caused one side of the specimen to curl tighter than the other.

The perpendicular fiber bilayer behaved as expected. The fibers constrained their surfaces so that they could only deform in directions perpendicular to fibers; fibers in one layer were perpendicular to the other layer. This resulted in bending on both the short and long axes. The arrangement of perpendicular fiber bilayers was analogous to how fibers in pine cone scales are structured; this design translated principles of how plants use fibers and structure to control and actuate movement.

The hydrogel bilayers discussed above are simply proof-of-concepts for ideas derived from how plants move that may be applied to different hydrogel actuator models using various hydrogels. The 1%-0.1% bilayer is proof that a hydrogel bilayer of different cross-linked densities can be synthesized and will curve in the direction of the less densely cross-linked network when dried. The random fiber bilayer demonstrates how the fibers can constrain shrinking rates and thus cause curvature towards the layer without fibers. The perpendicular fiber bilayer demonstrates how fibers in different layers that are approximately angled 90° to each other can cause bending due to the fact that they constrain deformation. These concepts could be the stepping stones to more complex hydrogel actuators.

Chapter 7 – FUTURE WORK

The bilayers that were created and tested are very basic proof-of-concept examples; there is a lot of research that needs to be done on how and why the movement of the actuators is affected. The hydrogel bilayers were tested by hanging on a string in order to constrain them as little as possible; however the location of the hole and the string seems to still have influenced their behavior by possibly contributing to cracking and influencing curvature. Future work could try to examine how the location of the hole and string affects the hydrogel bilayers by creating specimens that are circular in shape and placing the string directly through the middle. The circular geometry would also allow for the same axis in every direction and thus bending would likely be uniform. The circular geometry would be particularly interesting for the random fiber bilayer as the string often appeared to prevent the specimens from curling as much as they would have.

The effect of cracking on the bilayers could also be researched; quantifying exactly how these cracks affect the hydrogel bilayer curvature is important, especially when comparing the perpendicular fiber bilayers to the 1%-0.1% bilayers. Future research could also include examining how changing the cross-linking in bilayers by different orders of magnitudes affects the curvature as well as how changing the amount of cross-linking in the fiber bilayers affects curvature. In addition, researchers could look at making bilayers from tough hydrogels (discussed in section 2.3.5), some of which are even said to be "notch insensitive," which would likely be good for preventing cracks

[25, 28]. A continuation of this idea of making tough hydrogel bilayers is to make a hydrogel bilayer where one layer contains a DN or IPN and the other layer is simply one of the hydrogels used in the DN or IPN. Another area of research would be to apply these same plant movement concepts (varying cross-linking density bilayers and random fiber bilayers swelling/shrinking at different rates and perpendicular fibers constraining deformation to specific directions) to hydrogels that are stimuli-responsive (discussed in section 2.3.7). If the hydrogels were stimuli responsive for a volume change, the bilayers would no longer be dependent on a wet or dry environment but instead respond to another environmental stimulus, like light or temperature.

Another area of investigation would be to examine the exact mechanics of what is happening at the layer interface when synthesizing and drying the 1%-0.1% bilayers. Of particular importance is if any of the 0.1% layer solution is diffusing into the 1% layer as it rests on top of the 1% layer before UV radiation. There is also a question of whether or not any unreacted solution in the 1% layer is drawn up into the 0.1% solution as it rests on top of the 1% layer before UV radiation. Researchers could also investigate how to achieve more curvature when the bilayers are wet. One interesting avenue to do this might be to examine the effect of putting bubbles into the hydrogel layer, similar to how Wheeler et al. did in their experiment on a synthetic tree capable of transpiration (discussed in Section 2.3.8) [51].

Future examination could also look at the difference between fibers that are chemically bonded to the hydrogel and fibers that are not as well as fibers whose surfaces vary in roughness. Research could even include looking at how fiber stiffness and strength as well as the amount and distribution contribute to curvature. More fibers would

likely increase the curvature and a more even distribution would make the curvature more smooth and uniform for both random and perpendicular fiber bilayers. Perhaps a gradient effect in curvature might be achieved by a gradient effect in fiber distribution. In addition, fiber bilayers modeled after the perpendicular fiber bilayers could examine how changing the angle between the fibers from 90° to somewhere between 45° and 90° would change the bending and movement; it would be expected that some twisting would start to occur.

Rapid prototyping is an exciting area of further research for hydrogel actuators as it can allow for more complex shapes; it will be especially interesting if someone creates a way to place and align fibers within the hydrogel specimens. The most interesting of these technologies for this application is 2PP as it truly allows for the 3D creation of shapes instead of the layer by layer techniques seen in other rapid prototyping methods. Perhaps a swimming stimuli-responsive hydrogel actuator based on the wheat awn's movement principles seen Figure 2.6 could be created [4].

Finally, the movement of these actuators has only been studied going from wet to dry. Clearly, how the actuators go from dry to wet needs to be studied; how well they return to their original shape is critical. Furthermore, the hydrogel actuators should be cycled so that it can be determined how much fatigue occurs as they go from wet to dry and dry to wet repeatedly.

REFERENCES

1. Lee, Chi Hwan, Kim, Dong Rip, Cho, In Sun, William, Nemeth, Wang, Qi, and Xiaolin Zheng. Peel-and-Stick: Fabricating Thin Film Solar Cell on Universal Substrates. Scientific Reports, 2012, 2, 1-4.
2. Burgert, Ingo, and Peter Fratzl. Actuation Systems in Plants as Prototypes for Bioinspired Devices. Journal of the Royal Society Interface, 2009, 367, 1541-1557.
3. Booker, R.E. The reasons for the microfibril orientations in the tracheid cell walls of trees. In: Donaldson LA, Singh AP, Butterfield BG, Whitehouse LJ, editors. Recent advances in wood anatomy. Rotorua: New Zealand Forest Research Institute, 1996, 273-82.
4. Burgert, Ingo, and Peter Fratzl. Plants control the properties and actuation of their organs through the orientation of cellulose fibrils in their cell walls. Integrative and Comparative Biology, 2009, 49, 69-79.
5. Dunlop, John C., Weinkamer, Richard, and Peter Fratzl. Artful Interfaces within Biological Materials. Materials Today, 2011, 14, 70-78.
6. Li, Chensha, Liu, Ye, Huang, Xuezhen, and Hongrui Jiang. Direct Sun-Driven Artificial Heliotropism for Solar Energy Harvesting based on a Photo-Thermomechanical Liquid-Crystal Elastomer Nanocomposite. Advance Functional Materials, 2012, 22, 5166-5174.

7. Mousazadeh, Hossein, Keyhani, Alireza, Javadi, Arzhang, Mobli, Hossein, Abrinia, Karen, and Ahmad Sharifi. A review of principle and sun-tracking methods for maximizing solar systems output. Renewable and Sustainable Energy Reviews, 2009, 13, 1800-1818.
8. Volstad, Nina Louise, and Casper Boks. On the use of Biomimicry as a Useful Tool for the Industrial Designer. Sustainable Development, 2012, 20, 189-199.
9. Vincent, Julian F. V., Bogatyreva, Olga A., Bogatyrev, Nikolaj R., Bowyer, Adrian, and Anja-Karina Pahl. Biomimetics: its practice and theory. Journal of the Royal Society Interface, 2006, 3, 471-482.
10. Geim, A. K., Dubonos, S. V., Grigorieva, I. V., Novoselov, K. S., Zhukov, A. A., and S. Yu Shapoval. Microfabricated Adhesive Mimicking Gecko Foot-Hair. Nature Materials, 2003, 2, 461-463.
11. Esmon, C. Alex, Pedmale, Ullas V., and Emmanuel Liscum. Plant Tropisms: Providing the Power of Movement to a Sessile Organism. International Journal of Developmental Biology, 2005, 49, 665-674.
12. Sherry, R. A., and C. Galen. The mechanism of floral heliotropism in the snow buttercup, Ranunculus adoneus. Plant, Cell, and Environment, 21, 1998, 983-993.
13. Ehleringer, James, and Irwin Forseth. Solar Tracking by Plants. Science, 1980, 210, 1094-1098.
14. Cronlund, Sarah L., and Irwin N. Forseth. Heliotropic Leaf Movement Response to H+/ATPase Activation, H+/ATPase Inhibition, and K+ Channel Inhibition in Vivo. American Journal of Botany, 1995, 82, 1507-1513.

15. Morillon, Raphael, Lienard, David, Chrispeels, Maarten J., and Jean-Paul Lassalles. Rapid Movements of Plants Organs Require Solute-Water Cotransporters or Contractile Proteins. Plant Physiology, 2001, 127, 720-723.
16. Elbaum, Rivka, Stanislav, Gorb, and Peter Fratzl. Structures in the cell walls that enable hygroscopic movement of wheat awns. Journal of Structural Biology, 2008, 164, 101-107.
17. Das, Nilimanka. Preparation Methods and Properties of Hydrogel: A Review. International Journal of Pharmacy and Pharmaceutical Sciences, 2013, 5, 112-117.
18. Gulrez, Syed K. H., Al-Assaf, Saphwan, and Glyn O. Phillips. Hydrogels: Methods of Preparation, Characterisation, and Applications. Progress in Molecular and Environmental Bioengineering – From Analysis and Modeling to Technology Applications, Ed. Angelo Carpi. InTech, 2011. 117-150.
19. Billiet, Thomas, Vandenhaute, Mieke, Schelfhout, Jorg, Vlierberghe, Sandra Van, and Peter Dubruel. A Review of Trends and Limitations in Hydrogel-Rapid Prototyping for Tissue Engineering. Biomaterials, 2012, 33, 6020-6041.
20. Hoffman, Allan S. Hydrogels for Biomedical Applications. Advanced Drug Delivery Reviews, 2012, 64, 18-23.
21. Zhang, Xiaoyan, Guo, Xinglin, Yang, Shuguang, Tan, Shuaixia, Li, Xiaofeng, Dai, Hongjun, Yu, Xiaolan, Zhang, Xiaoli, Weng, Ning, Jian, Bin, and Jian Xu. Double-Network Hydrogel with High Mechanical Strength Prepared from Two Biocompatible Polymers. Journal of Applied Science, 2009, 112, 3063-3070.

22. Schacht, E. H. Polymer chemistry and hydrogel systems in the Third International Conference on Radiotherapy Gel Dosimetry, 2004.
23. Anseth, Kristi S., Bowman, Christopher N., and Lisa Brannon-Peppas. Mechanical Properties of Hydrogels and their Experimental Determination. Biomaterials, 1996, 17, 1647-1657.
24. Paul Calvert. Hydrogels for Soft Machines. Advanced Materials, 2009, 21, 743-756.
25. Peak, Charles W., Wilker, Jonathan J., and Gudrun Schmidt. A Review on Tough and Sticky Hydrogels. Colloid and Polymer Science, 2013, 291, 2031-2047.
26. Gong, Jian Ping, Katsuyama, Yoshinori, Kurokawa, Takayuki, and Yoshihito Osada. Double Network Hydrogels with Extremely High Mechanical Strength. Advanced Materials, 2003, 15, 1155–1158.
27. Wang, Xuezhen, Wang, Huiliang, and Hugh R. Brown. Jellyfish Gel and its Hybrid Hydrogels with High Mechanical Strength. Soft Matter, 2011, 7, 211–219.
28. Sun, Jeong-Yun, Zhao, Xuanhe, Illeperuma, Widusha R. K., Chaudhuri, Ovijit, Oh, Kyu Hwan, Mooney, David J., Vlassak. Joost J., and Zhigang Suo. Highly Stretchable and Tough Hydrogels. Nature, 2012, 489, 133–136.
29. Kopeček, Jindřich. Hydrogel Biomaterials: A Smart Future?. Biomaterials, 2007, 28, 5185-5192.
30. Liu, Jiaqi, Chen, Caifeng, He, Changcheng, Zhao, Jing, Yang, Xiaojing, and Huiliang Wang. Synthesis of Graphene Peroxide and Its Application in Fabricating Super Extensible and Highly Resilient Nanocomposite Hydrogels. ACS Nano, 2012, 6, 8194-8202.

31. Wang, Qiang, Hou Ruixia, Cheng, Yajun, and Jun Fu. Super-Tough Double Network Hydrogels Reinforced by Covalently Compositing with Silica-Nanoparticles. Soft Matter, 2012, 8, 6048–6056.
32. Xu, Kun, Tan, Ying, Chen, Qiang, An, Huiyong, Li, Wenbo, Dong, Lisong, and Pixin Wang. A Novel Multi-Responsive Polyampholyte Composite Hydrogel with Excellent Mechanical Strength and Rapid Shrinking Rate. Journal of Colloid and Interface Science, 2010, 345, 360–368.
33. Kohzo Ito. Slide-Ring Materials using Topological Supramolecular Architecture. Current Opinion in Solid State and Matter Science, 2010, 14, 28-34.
34. Kohzo Ito. Novel Entropic Elasticity of Polymeric Materials: Why is Slide-Ring Gel so Soft? Polymer Journal, 2012, 44, 38–41.
35. Mitsuhiro Shibayama. Structure–Mechanical Property Relationship of Tough Hydrogels. Soft Matter, 2012, 8, 8030–8038.
36. Haque, Md. Anamul, Kurokawa, Takayuki, and Jian Ping Gong. Super Tough Double Network Hydrogels and their Applications as Biomaterials. Polymer, 2012, 53, 1805-1822.
37. Han, Jingquan, Lei, Tingzhou, and Qinglin Wu. High-Water-Content Mouldable Polyvinyl Alcohol-Borax Hydrogels Reinforced by Well-Dispersed Cellulose Nanoparticles: Dynamic Rhealogical Properties and Hydrogel Formation Mechanism. Carbohydrate Polymers, 2014, 102, 306-316.
38. Haque, Md. Anamul, Kamita, Gen, Kurokawa, Takayuki, Tsujii, Kaoru, and Jian Ping Gong. Unidirectional Alignment of Lamellar Bilayer in Hydrogel: One-

Dimensional Swelling , Anisotropic Modulus, and Stress-Strain Tunable Structural Color. Advanced Materials, 2010, 22, 5110-5114.

39. Haque, Md. Anamul, Kurokawa, Takayuki, Kamita, Gen, and J. Ping Gong. Lamellar Bilayers as Reversible Sacrificial Bonds to Toughen Hydrogel: Hysteresis, Self-Recovery, Fatigue Resistance, and Crack Blunting. Macromolecules, 2011, 44, 8916-8924.
40. Nakayama, Atsushi, Kakugo, Akira, Gong, Jian Ping, Osada, Yoshihito, Takai, Mitsuo, Erata, Tomoki, and Shin Kawano. High Mechanical Strength Double-Network Hydrogel with Bacterial Cellulose. Advanced Functional Materials, 2004, 14.11, 1124-1128.
41. Agrawal, Animesh, Rahbar, Nima, and Paul D. Calvert. Strong Fiber-Reinforced Hydrogel. Acta Biomaterialia, 2013, 9, 5313-5318.
42. Zhang, Shuming, Liu, Xi, Barreto-Ortiz, Sebastian F., Yu, Yixuan, Ginn, Brian P., DeSantis, Nicholas A., Hutton, Daphne L., Grayson, Warren L., Cui, Fu-Zhai, Korgel, Brian A., Gerecht, Sharon, and Hai-Quan Mao. Creating Polymer Hydrogel Microfibres with Internal Alignment via Electrical and Mechanical Stretching. Biomaterials, 2014, 35, 3243-3251.
43. Messing, Renate, and Annette M. Schmidt. Perspectives for the Mechanical Manipulation of Hybrid Hydrogels. Polymer Chemistry, 2011, 2, 18-32.
44. Kirschner, Chelsea M. and Kristi S. Anseth. Hydrogels in Healthcare: From Static to Dynamic Material Microenvironments. Acta Materialia, 2013, 61.3, 931-944.
45. "Photoisomerization." *Encyclopaedia Britannica. Encyclopaedia Britannica Online Academic Edition*. Encyclopædia Britannica Inc., 2014. Web. 02 Apr.

2014. <http://www.britannica.com/EBchecked/topic/457736/photochemical-reaction/277515/Photoisomerization >.

46. Sidorenko, Alexander, Krupenkin, Tom, Taylor, Ashley, Fratzl, Peter, and Joanna Aizenberg. Reversible Switching of Hydrogel-Actuated Nanostructures into Complex Micropatterns. Science, 2007, 315, 487-490.
47. He, Ximin, Aizenberg, Michael, Kuksenok, Olga, Zarzar, Lauren D., Shastri, Ankita, Balazs, Anna C., and Joanna Aizenberg. Synthetic Homeostatic Materials with Chemo-Mechano-Chemical Self-Regulation. Nature, 2012, 487, 214-218.
48. Maeda, Shingo, Hara, Yusuke, Nakamaru, Satoshi, and Shuji Hashimoto. Design of Autonomous Gel Actuators. Polymers, 2011, 3, 299-313.
49. Medhavi, Amit. Peristaltic Pumping of a Non-Newtonian Fluid. Applications and Applied Mathematics: An International Journal, 2008, 3, 137-148.
50. Latham, Thomas Walker. Fluid Motion in a Peristaltic Pump. MS Thesis, MIT, Cambridge, MA, 1966.
51. Wheeler, Tobias D., and Abraham D. Stroock. The transpiration of water at negative pressures in a synthetic tree. Nature, 2008, 455, 208-212.